SEQUESTRATION OF HYDROPHOBIC ORGANIC CONTAMINANTS IN

SEDIMENTS

A dissertation

Submitted to the Graduate Faculty of the Louisiana State University and
Agricultural and Mechanical College
In partial fulfillment of the
Requirements for the degree of
Doctor of Philosophy

In

The Department of Chemical Engineering

By

Yunzhou Chai

B.S. Xiamen University, China, 1997

December 2004

ACKNOWLEDGEMENTS

TABLE of CONTENTS

LIST OF TABLES

LIST OF FIGURES

ABSTRACT

CHAPTER 1 INTRODUCTION

1.1 Motivation and relevance of the problem

Soils and sediments acting as natural sorbents are the ultimate sink for many hydrophobic organic contaminants (HOCs). The availability issue of these HOCs has become the focus of more and more researchers in that realistic endpoints for remediation processes depend highly on the availability of these HOCs. It might be acceptable to leave the residual contaminants intact in the sediment if the residual fraction of the contaminant is hardly available. As a result, significant cost reduction will be achieved for remediation while little or no increase in risk to the environment will be caused.

Availability of contaminants includes physical availability and biological availability. The ability of sediment-bound contaminants to partition or desorb to a mobile phase or the extractability of sediment-bound contaminants using a solvent or a sorbent defines physical availability of contaminants. The biological availability describes the exposure, uptake and ultimate risk of sediment-bound contaminants to receptor organisms and biodegradation of sediment-bound contaminants by microorganisms. To a great degree, physical availability of sediment-bound contaminants controls its bioavailability because the partitioning of a contaminant between the solid and water phases is a key indicator of the potential for exposure and risk (Reible and Demnerova, 2001). Thus, sorption and desorption of HOCs in natural sorbents are critical processes determining the transport, fate and bioavailability of HOCs in the environment although enormous uncertainty is involved in the quantification of the risk assessment.

The equilibrium distribution of HOCs between sediment/soil and water has been considered to be a linear and reversible partitioning process, which suggests that a hundred

percent of sediment/soil-associated contaminant is available to partitioning or biological receptors in the environment. The reported desorption resistance (or hysteresis) is not explainable by the conventional linear partitioning model. This phenomenon suggests that only a fraction of the total contaminants may be available or readily available to partitioning or receptors. The fraction that is unavailable or not readily available is often referred to as the desorption-resistant fraction of contaminants or sequestered contaminants. The sequestration of contaminants into organic matter in sediments/soils has been ascribed to the effects of different sorbing nature of various soil/sediment organic matrices and conformational or other changes of the contaminants in the matrices.

Although various research groups have developed models in an attempt to understand the physics and chemistry behind the sequestration of contaminants in natural sorbents, no model is able to predict *a priori* the contaminant concentration in the aqueous phase in a contaminated sediment system influenced by a desorption resistant fraction of contaminants. In order to establish realistic endpoints for remediation processes, the physical chemical mechanisms that govern sequestration and release of contaminants in sediments/soils must be fully understood. Therefore, the proposed work will focus on understanding the mechanisms for the sequestration of hydrophobic organic contaminants in natural sorbents and establishment of a predictive model to delineate sorption/desorption behavior of hydrophobic organic contaminants in natural sorbents in the environment.

1.2 Background and literature review

1.2.1 Sequestration phenomena of contaminants in soils and sediments

In naturally occurring systems most hydrophobic organic contaminants are associated with sediment or soil, sorbed primarily to the sediment/soil organic matter. Sorption and desorption of HOCs affect contaminant fate, toxicology and the efficiency of most remediation technologies. In fate, risk, and remediation models, sorption and desorption are commonly described as a linear and reversible partitioning process by the following equation (Karickhoff et al., 1979).

$$C_s = K_p \cdot C_w \qquad (1.1)$$

Where C_s (mg/kg) is the contaminant concentration associated with the soil or sediment phase, C_w (mg/L) is the aqueous concentration, and K_P (L/kg) is the equilibrium sediment/soil-water partition coefficient. Since most contaminants are believed to reside in soil/sediment organic matter (SOM) in natural sorbents (Karickhoff, 1981; Di Toro et al., 1991), organic carbon normalized sediment water partition coefficient K_{oc} is more frequently used, which is related to K_p by equation 1.2,

$$K_p = K_{oc} f_{oc} \qquad (1.2)$$

where f_{oc} is the mass fraction of organic carbon in a sediment/soil, and K_{oc} relates to octanol-water partition coefficient (K_{ow}) or aqueous solubility (*Sol*) of contaminant as measures of hydrophobicity. The K_{oc} has been correlated with octanol water partition coefficient or solubility by relationship of the form:

$$\log K_{oc} = a_1 \cdot \log K_{ow} + b_1 \qquad (1.3)$$

or

$$\log K_{oc} = a_2 \cdot \log Sol + b_2 \qquad (1.4)$$

where a1, b1 and a2, b2 are constants (Chiou et al. 1979; Karickhoff et al. 1979; Karickhoff, 1981, 1984; Means et al., 1980, 1982; Schwarzenbach and Westall, 1981; Schellenberg et al., 1984; Chin and Weber, 1989). Selected empirical correlations to estimate K_{oc} from K_{ow} are summarized in table 1.1.

Table 1.1 Empirical Correlations to estimate organic carbon normalized partition coefficient

Compound Class	a_1	b_1	Reference
PAHs, Chlorinated HOCs	1.0	-0.21	Karickhoff et al., 1979
PAHs, Amino- and Carboxy- substituted PAHs	1.0	-0.317	Means et al., 1980
PAHs	0.989	-0.346	Karickhoff, 1981
PAHs, Chlorinated HOCs	0.72	+0.49	Schwarzenbach and Westall, 1981
Neutral chlorinated phenols	0.82	+0.02	Schellenberg et al., 1984

Equation 1.1 works well to describe the bulk of contaminant sorption and desorption, especially for natural sorbents contaminated for days to weeks, but it has been proven that equation 1.1 does not appropriately describe partitioning of desorption-resistant fraction of contaminants. It has been observed that the desorption of contaminants from natural sorbents to be biphasic, which suggests a relatively rapid release and degradation of organic contaminants in soils and sediments initially followed by a period of slow or very slow change, there is always a significant fraction of sorbed contaminant which is resistant to

desorption. This fraction may persist much longer (Karickhoff, 1980; Cornelissen, 2001; Hawthorne, 2001) and be less available to organisms or other receptors (White, 1998; Lee, 2001; Lu, 2003a; Lu, 2003b) than would be expected by the reversibly sorbed contaminants. It has been reported that desorption resistance increases and bioavailability decreases with the contaminant-sediment contact time, which is commonly referred to as "aging" effect (Pignatello, 1993; Ma, 1993; Hatzinger, 1995; McGroddy, 1996; White, 1997; White, 1999; Lee, 2001; Lu, 2003a). It also has been observed in the field that polycyclic aromatic hydrocarbons (PAHs) sorbed to sediments more than predicted by the $f_{oc}*K_{oc}$ model (McGroddy, 1995; Jonker, 2000).

Phenomenologically, the biphasic desorption kinetics can be modeled using a two-compartment first-order kinetic model (Karickhoff, 1980; Hawthorne, 2001),

$$\frac{S_t}{S_0} = 1 - Fe^{-k_1 t} - (1 - F)e^{-k_2 t} \tag{1.5}$$

Where t is time (days), S_t is the mass of contaminant removed by sorbent, and S_0 is the total initial mass of contaminant in sediment; S_t/S_0 is the fraction of contaminant released after time t. F is the fraction of contaminant released quickly; (1-F) is the fraction of contaminant released slowly. k_1 and k_2 are the first-order rate constants describing the fast and slowly releasing fractions respectively (day^{-1}). Similarly, Cornelissen et al. proposed a three compartment first-order desorption kinetic model to fit their data (Cornelissen, 2001). These empirical kinetic models are able to fit the experimental data successfully, however, they do not provide information on the mechanisms behind this biphasic desorption behavior.

Various models and interpretations have been proposed to explain the biphasic desorption behavior of HOCs in natural sorbents. Although they take various mathematical

forms and different ways of interpretation, they all assume that the sediment organic matter is heterogeneous and composed of a desorption-resistant fraction and a reversibly sorbed fraction. A summary of the basic characteristics and implications of these interpretations is given below.

1.2.2Different interpretations of the sequestration behavior

Ghosh et al. applied microscopic direct observation on Milwaukee harbor sediment particles with the aid of IR spectrophotometry and scanning electron microscope (SEM). They found some "black" particles that are the second most abundant particles after "silica" in the sediment. They identified the "black" particles containing high organic carbon content as coal or coal/wood-derived component in the sediment by petrography analysis (Ghosh et al, 2000).

Ghosh et al. separated Milwaukee Harbor sediment into two broad categories--"light" and "heavy" fractions, by wet sieving and density separation using a cesium chloride solution with a specific gravity of 1.8 (Ghosh et al, 2000). The light fraction, basically black particles, comprised primarily of coal- and wood-derived particles. After further separation, it turned out that the light fraction comprised predominantly of coal-derived particles (Ghosh et al, 2001).

A cryomicrotome technique and microprobe two-step laser desorption/laser ionization mass spectrometry ($\mu L^2 MS$) were utilized to investigate the cross sectional distribution of PAHs in these coal-derived and silica particles by Gillette et al. (1999), results suggested that most PAHs are concentrated in near external surface regions of these coal-derived particles indicating near surface sorption mechanisms. Given that the presence of PAHs was likely due to historical contamination over decades, slow diffusion of the contaminants was proposed to

explain and model the desorption of contaminants from those coal-derived particles. The "rind" model, with an initial PAH concentration in the outer regions of the particle, predicted a very slow long-term release with 40% PAH remaining even after 100 years (Ghosh et al., 2001).

Weber et al. classify the organic carbon that can be oxidized by low-temperature persulfate oxidation "soft carbon", and by high-temperature combustion with pure oxygen "hard carbon" (Weber et al., 1992). They observed that the "hard carbon" fraction increases with the geological age of the organic matter. Elemental analysis and solid-state 13C-NMR spectra reveal that the O/C atomic ratio of the sediment organic matter decreases with increased geological age of the sediment (Huang, 1997). They also observed that the sorption affinities of these materials for phenanthrene as well as their respective isotherm nonlinearity and hysteresis correlate inversely with the O/C atomic ratio. They found that samples containing more physically condensed and chemically reduced sediment organic matter matrices exhibited greater solute affinity, more nonlinear sorption equilibria, and more pronounced hysteresis (Huang, 1997).

Weber et al. proposed a composite model--Distributed Reactivity Model (DRM), which describes sorption isotherm as a combination of a series near-linear absorption reactions and nonlinear adsorption reactions (Weber et al., 1992). The sorption isotherm is expressed by the following equation,

$$q_s = x_l K_{D_r} C_w + \sum_{i=1}^{m} (x_{nl})_i K_{F_i} C_w^{n_i}$$
(1.6)

Where, x_l: summed mass fraction of solid phase exhibiting linear sorption, K_{D_r}: mass averaged partition coefficient for linear portion, $(x_{nl})_i$: mass fraction of the ith nonlinearly

sorbing component, and m is usually 1 or 2. They believed that the entrapment of sorbing molecules within the condensed phase sediment organic matter matrices contributes to sorption-desorption hysteresis (Huang and Weber, 1997a).

Xing et al. proposed Dual Mode Model (DMM) to interpret their experimental data by introducing polymer theory in which the sediment organic matter was classified into two categories--"glassy" and "rubbery" phases (Xing et al., 1996). They postulated that contaminants are sorbed in rubbery SOM by linear partitioning and in glassy SOM by partitioning and hole-filling processes. The model was expressed by the following equation:

$$s = k_p c + \sum_{i=1}^{n} \frac{s_i^0 b_i c}{1 + b_i c} \tag{1.7}$$

where k_p: linear partition coefficient, b_i: affinity constant, s_i^0: maximum capacity, n: n unique holes. Similar to DRM, sorption hysteresis is ascribed to the hole-filling process in the "glassy" phase (Xing and Pignatello, 1997). The difference between DRM and DMM is that Freundlich type of isotherm was used in DRM to describe nonlinear contribution but Langmuiran type of isotherm was used in DMM. Essentially, it does not make any difference in that the Freundlich isotherm can be expressed as the sum of a series Langmuiran isotherms.

Rockne et al. investigated desorption of PAHs from whole and fractionated sediments, one domain and two domain diffusion models were utilized to fit their experimental data for more hydrophobic and less hydrophobic PAHs respectively (Rockne et al., 2002; Shor et al., 2003). Although model fitting was successful for their desorption data, the assumption that PAHs were initially uniformly distributed throughout sediment aggregates was not appropriate in that microscopic observations showed that PAHs only resided in a thin layer near external surface of the coal-derived particles in the sediment (Ghosh et al., 2001).

Kan et al. utilized successive batch sorption/desorption experiments to investigate the desorption reversibility of hydrophobic organic contaminants from natural sorbents (Kan et al., 1994; Kan et al., 1997; Kan et al., 1998; Chen et al., 2000). A maximum irreversible concentration, q_{max}^{irr}, was observed for certain contaminant/sediment system. Before q_{max}^{irr} is reached, 30-50% of the sorbed contaminants resides in the "irreversibly" sorbed compartment and the rest resides in the labile and reversible compartment. The "irreversibly" sorbed amount varied with initial concentration available for sorption and the amount in the "irreversibly" sorbed compartment increases linearly with the number of adsorption steps. After q_{max}^{irr} is reached, adsorption/desorption becomes "reversible". If the "reversible" portion is removed, the "irreversible" portion is at equilibrium with aqueous phase, but equilibrium concentration in aqueous phase is much lower than would be predicted with conventional partitioning theory. They found that, for most compounds, q_{max}^{irr} is approximately $10^{3.8}$ multiplied by the organic carbon content of the sediment, and that organic carbon normalized partition coefficient for irreversible compartment, k_{oc}^{irr}, is constant for different compounds and sediments studied, which is $10^{5.53 \pm 0.48}$ (Kan et al., 1998). The following biphasic isotherm model is proposed to fit the experimental data,

$$q = K_{OC} \times OC \times C + \frac{K_{OC}^{irr} \times OC \times q_{max}^{irr} \times f \times C}{q_{max}^{irr} f + K_{OC}^{irr} \times OC \times C} \tag{1.8}$$

where f is the fraction of the irreversible compartment that is filled at the time of exposure, f takes its value from 0 to 1, f is 1 when the initial aqueous concentration is greater than a half of the solubility of the compound in water. The isotherm consists of two terms, a linear term to represent reversible sorption and a Langmuirian-type term to represent irreversible

9

sorption. After about 1-3 days of contact time, all laboratory sorption and desorption data could be modeled using the above isotherm equation.

They postulated that the observed phenomenon might be due to the occlusion of desorption resistant contaminants from desorption by cooperative conformational changes of the organic phase during the sorption process (Kan et al., 1997). The conformational rearrangement of the soil/sediment organic matter in the presence of adsorbed contaminants could cause the chemical environment of the adsorbate to be different and hence be the source of the desorption resistance. The biphasic model fit their experimental data successfully and explained the biphasic desorption phenomena, but no evidence was provided to defend the hypothesis of rearrangement of organic matter in sediment.

Elevated partition coefficients other than predicted from organic carbon normalized partition coefficients for PAHs have been observed in field sediments. Gustafsson et al. quantified the "black carbon" (e.g. soot and chars etc.) content in the sediment by thermal oxidation method ("black carbon" content is the organic carbon content of the sediment sample after combustion under 375°C) and included the contribution of "black carbon" to understand the elevated partition coefficient (Gustafsson et al., 1997). The following isotherm was proposed

$$C_s = f_{OC}K_{OC}C_W + f_{BC}K_{BC}C_W{}^n \tag{1.9}$$

where K_{BC} is "black carbon" normalized distribution coefficient which is much higher than that of ordinary sediment organic matter. In this way, it is easy to understand the elevated partition coefficient but no explanation was provided to explain aging effects. Other researchers have also reported that sediment organic carbon particles such as coal, coke, and soot have extremely high partition coefficients as a measurement of sorption capacity. Ghosh

et al. (2003) collected organic carbon normalized partition coefficients values for various particles from literature spanning about 3 logarithmic units from 4 to 7 (Karapanagioti, et al., 2000; Walters and Luthy, 1984; Gustafsson and Gschwend, 1997; Gaboriau and Saada, 2001; Chiou et al., 1998; Karickhoff et al., 1979; Salloum et al., 2002). Jonker and Koelmans (2002) reported that sorption of PAHs to different soot and soot-like materials was over 1000 times as strong as the sorption to amorphous sediment organic carbon as indicated by those elevated partition coefficients.

The aging effect of hydrophobic organic contaminants in sediment has been attributed to the slow diffusion of contaminants in the condensed phase organic matter in sediment. Pignatello et al. investigated elution of aged and freshly added herbicides from a soil and they found that the mobility of the added herbicide was much greater than the native herbicide. They argued that the diffusion of herbicide in the slow sorption compartment in soil is probably the cause to the aging effect (Pignatello et al., 1993). Particle scale direct observation by Ghosh et al. reveals that PAHs distribute mostly in the outer region of the coal-derived particles (Ghosh et al., 2001), which indicate that it takes a long time for contaminants to migrate into the condensed phase particles through diffusion and directly support the argument that the aging effect might results from diffusion of contaminants in certain fraction of the organic matter in sediment.

1.2.3 Summary

The following ideas can be extracted from the above-mentioned models and interpretations:

1. Biphasic desorption phenomena results from organic carbon heterogeneity. Sediment/soil organic matter can be classified into two general categories as

amorphous and condensed phase organic matter. Denotations like "coal-derived" particle, "soot carbon", "black carbon" and "hard carbon" have been used to refer to condensed phase organic carbon while natural organic matter has been used to refer to amorphous organic carbon.

2. Condensed phase organic carbon exhibits elevated organic carbon normalized partition coefficient, which indicates greater sorption capacity and slower sorption/desorption rates.

3. Desorption resistance of organic contaminants and aging effect result from the slow diffusion of contaminants in the condensed phase organic carbon.

Although these basic ideas are widely acknowledged to explain the biphasic sorption and desorption behaviors of HOCs in sediments and soils, nobody, however, has ever utilized these basic ideas and mathematical models to predict quantitatively the availability of sequestered contaminants in sediments including the desorption resistance, apparent partition coefficients and aging effects. It is, thus, necessary to develop a predictive model so that the model can be used to estimate *a priori* the availability of sequestered contaminants in soils and sediments when developing realistic regulations and remediation endpoints for contaminated soils and sediments.

1.3 Objectives of present study

1.3.1 Overall objectives

The proposed research is directed toward understanding the mechanisms for the sequestration of hydrophobic organic contaminants (HOCs) in natural sorbents and establishing a predictive model of sorption/desorption behavior of hydrophobic organic

contaminants onto/from natural sorbents in the environment. The proposed studies will utilize both lab-inoculated and field contaminated sediments as test media. These studies will focus on polynuclear aromatic hydrocarbons (PAHs) in that they are common sediment contaminants and present a wide range of hydrophobicities and toxic characteristics.

1.3.2 Specific objectives and approaches

1.3.2.1 Development of a predictive model to address sorption/desorption behavior of HOCs onto/from soils and sediments

Hypotheses: (1) Variations in desorption rate and extent from contaminated sediments is associated with soil organic matter heterogeneity. Greater sorption capacity (more limited desorption) and reduced rates of sorption and desorption are associated with condensed phase carbon formed from natural processes over long periods of time or by combustion processes over shorter time periods. (2) Although there exists a continuum of organic matter quality and resulting sorption capacities and rates, the sorption and desorption phenomena can be described by considering only two broad classes, an amorphous phase in which sorption and desorption is relatively fast and reversible and a condensed phase in which sorption and desorption is relatively slow and for which phase exhibits greater capacity than the amorphous phase. (3) The condensed phase is approximately described by each of the characterizations found in the literature, that is as hard carbon, as glassy polymer, as diagenetically aged carbon, as soot carbon, as coal-derived particle, and black carbon, etc; and these phases are roughly equivalent. (4) The sorption and desorption to the amorphous carbon can be described by diffusion in a porous matrix with equilibrium partitioning described by the organic carbon based partition coefficient as measured in

short-term sorption experiments. (5) The sorption and desorption to the condensed phase carbon can be described by much slower solid phase diffusion and with equilibrium partitioning measured experimentally to be higher than the organic carbon based partition coefficient.

1.3.2.2 Validation of the model by doing short-term experiments

a. Determination of the relationship between desorption resistance of freshly inoculated contaminants and the heterogeneity of organic matter in soils and sediments, testing the model to determine whether the model is able to predict the biphasic desorption kinetics and the relationship between desorption resistance and heterogeneity of sediment organic matter.

   Hypothesis: Contaminants residing in sediment with higher condensed phase organic carbon content (foc^c/Toc) exhibits greater desorption resistance, the model is able to predict this relationship and the biphasic desorption kinetics.

b. Determination of relationship between desorption resistance of "aged" inoculated contaminants (aging effect) and the heterogeneity of organic matter in soils and sediments, testing the ability of the model to predict aging effect.

   Hypothesis: Aging effect for sediment with higher condensed phase organic carbon content is more significant than that of sediment with less condensed phase organic carbon content, the model is able to predict aging effect of contaminant in sediments with different hard organic carbon contents.

c. Evaluation of the effects of slow kinetics of contaminants in condensed phase organic carbon on measured apparent partition coefficient of contaminants in sediments, testing

the ability of the model to predict the elevated apparent partition coefficient for the desorption-resistant contaminant.

Hypothesis: Relatively short equilibration time for partition coefficient measurement is not long enough to reach real equilibrium; the model is able to predict the elevated apparent partition coefficient for the desorption-resistant contaminant.

d. Determination of the effects of organic matter heterogeneity on contaminants distribution and availability in fractionated sediments

Hypothesis: Distribution and availability of contaminants in different sediment fractions is related to the characteristics of organic carbon matrices in those fractions.

1.4 Overview

This dissertation consists of seven chapters. The main contents of each chapter are briefed below. Chapter 1 summarizes the current understanding of the fundamental aspects of sorption and desorption processes involved in the sequestration and release of HOCs by soils/sediments. Chapter 2 covers the availability of HOCs in laboratory-inoculated sediments and field-contaminated sediment. Correlation of desorption resistance and condensed phase carbon content will be discussed. Chapter 3 describes the size and density separation for sediments, including contaminant distribution and sediment mass distribution in sediment fractions, availability of contaminant in different sediment fractions. Chapter 4 characterizes the observations obtained on coarse particles from field-contaminated sediment. Chapter 5 contains the modeling activities. Processes including desorption, partition and aging of contaminants in sediment will be modeled and discussed. Chapter 6 summarizes major conclusions in this research and recommendations for future work.

CHAPTER 2 AVAILABILITY OF CONTAMINANTS IN SEDIMENTS WITH DIFFERENT CONDENSED PHASE ORGANIC CARBON CONTENTS

2.1 Introduction

Recent research has revealed that the availability of sediment-associated hydrophobic organic contaminants but not the total sediment-associated contaminants is critical in defining exposure, uptake and ultimate risk of contaminants to receptor organisms in the environment. Availability of contaminants includes physical availability and biological availability. The ability of sediment-bound contaminants to partition or desorb to a mobile phase or the extractability of sediment-bound contaminants using a solvent of a sorbent defines physical availability of contaminants. The biological availability describes the exposure, uptake and ultimate risk of sediment-bound contaminants to receptor organisms and biodegradation of sediment-bound contaminants by microorganisms. To a great degree, physical availability of sediment-bound contaminants controls its bioavailability because the partitioning of a contaminant between the solid and water phases is a key indicator of the potential for exposure and risk (Reible and Demnerova, 2001).

In fate, risk, and remediation endpoints evaluation of sediment-associated hydrophobic organic contaminants, total solid phase concentration was used assuming linear partition model (Karickhoff et al., 1979), which suggests that a hundred percent of the sediment-associated contaminants is available to partition into mobile phase. There is increasing evidence, however, to show that a fraction of the sediment-bound contaminants is not easily desorbed which results in reduced availability of the desorption-resistant fraction of

contaminant (Robinson et al., 1990; Alexander, 1994; Loonen, et al., 1994; Cornelissen et al., 1998; Opdyke and Loehr, 1999). Thus, the linear, reversible partitioning model (Karickhoff et al., 1979) is no longer appropriate to describe desorption of the resistant compartment, and biphasic models (Karickhoff, 1980; Hawthorne, 2001) have been proposed to describe the biphasic desorption phenomenon which exhibits a rapid release of a reversible labile fraction followed by a slow release of the resistant fraction.

The desorption-resistance has been ascribed to the heterogeneity of organic matter present in sediments. In addition to the amorphous natural organic matter, condensed phase carbon, similar names as hard carbon, soot, black carbon, glassy polymer, coal-derived particle etc., has been widely found in field-contaminated sediments and been postulated to be responsible for the desorption resistance of contaminants in sediments (Weber et al., 1992; Huang and Weber, 1997a; Gustafsson, et al., 1997; Ghosh, et al, 2001; Kan et al., 1998; Xing et al., 1996; Xing and Pignatello, 1997; Rockne et al., 2002). The condensed phase carbon has been considered to be the source of desorption resistance in that it exhibits extremely high sorption capacity as indicated by elevated partition coefficient (Gustafsson and Gschwend, 1997; Ghosh et al., 2003), and it is highly reduced and condensed in form so that the diffusion rate of contaminants in this phase is extremely slow (Ghosh et al., 2001). The condensed phase carbon has been operationally defined by the fraction of organic carbon remaining after sediment was combusted under 375°C (Gustafsson et al., 1997).

This chapter is directed toward characterizing the relationship between the desorption-resistant phenomena and sediment organic matter quality specifically condensed phase carbon content.

Two laboratory-inoculated sediments, Bayou Manchac sediment and University Lake sediment, were inoculated with phenanthrene, a hydrophobic polycyclic aromatic hydrocarbon as well as a significant pollutant in contaminated sediment to conduct the study. The desorption kinetics were determined using XAD2, a nonpolar sorbent, as an infinite sink to remove phenanthrene from the inoculated sediment. The desorption isotherms of phenanthrene were established based on the measured sediment concentration and pore water concentration at the completion of measurement of apparent sediment–water partition coefficients for a series of desorbed sediments. The desorbed sediments in which desorption-resistant contaminant consisted various fraction of the remaining contaminant were prepared by washing the laboratory-inoculated sediment with an isopropanol/electrolyte solution (v/v 1:1) to remove reversibly sorbed contaminant (Lu, 2003).

Two field-contaminated sediments, Utica Harbor sediment and Rouge River sediment, were also used in this study. The fast desorption fraction, as characterized by the fraction removed by XAD2 in 20 hours, of a number of PAHs in the sediments were determined. The apparent sediment–water partition coefficients of these PAHs in the sediments before and after the sediments were subjected to XAD2 treatment were determined.

2.2 Materials and methods

2.2.1 Contaminant

Phenanthrene (PHE, 98% purity), used as trace contaminant in this study to inoculate Bayou Manchac and University Lake sediments, was purchased from Aldrich Chemical Corporation (Milwaukee, WI, USA).

2.2.2Sediments

Two clean sediments, Bayou Manchac sediment and University Lake sediment, were used in the experiments to inoculated phenanthrene as trace contaminant. Bayou Manchac sediment was collected from Bayou Manchac, a fresh water bayou in Baton Rouge, Louisiana, in 1998 and University Lake sediment was collected from University Lake, Baton Rouge, Louisiana, in 1999. Contaminants in these sediments were analyzed according the procedure described in section 2.2.6 and results showed that these sediments were originally free of contaminants. After collection, these sediments were coarsely sieved to remove twigs, leaves, etc., and then they were passed through a 2mm sieve to remove debris and large particles.

Two field-contaminated sediments, Utica Harbor sediments and Rouge River sediment, were also used in this research. Utica Harbor sediment was collected from Utica Harbor, NY, Rouge River sediment was collected from Rouge River, MI.

All sediments were sieved through 2 mm sieves before used for the experiment and were stored in room temperature in tightly sealed barrels with overlying water to avoid air-drying.

2.2.3Sediment inoculation

The sediments after sieving were spiked with the tracer chemical as model contaminant using the shell-coating procedure employed by Thoma (1994). Sediments were inoculated at saturation concentrations of phenanthrene (PHE), which were estimated from the linear correlation 1.1 and 1.2 with maximum possible aqueous concentration that is water solubility of the model contaminant, as shown in equation 2.1,

$$C_S = K_{OC} \cdot f_{OC} \cdot Sol. \tag{2.1}$$

Where *Sol.* is the aqueous solubility of the compound. The saturation concentration of phenanthrene in Bayou Manchac sediment and University Lake sediment were estimated to be approximately 380mg and 1640mg PHE per kilogram dry sediment.

The sediment inoculation procedures were described as the following steps:

First) the pre-weighed model contaminants, phenanthrene in this case, were dissolved in hexane and then transferred into the inoculation vessel (4-L glass jar).

Second) Hexane was evaporated under a stream of high pure nitrogen as the inoculation vessel was being rotating and crystals of the solid model contaminant were uniformly deposited on the internal wall of the inoculation vessel as hexane evaporated.

Third) Weighed wet sediment was added into the inoculation vessel, water might be added to adjust the water content of the sediment to 50% to achieve better mixing when tumbling.

Fourth) Approximately 3000µg/g sodium azide was also added to the inoculation vessel to inhibit bacterial metabolism of the contaminants during tumbling. Results have shown that this concentration of sodium azide was sufficient to avoid degradation as indicated by the ability to maintain constant sediment concentration and satisfied mass balances during the tumbling.

Fifth) The inoculation vessel was tumbled for approximately five weeks at an axial rotation rate of 5-10 rpm on a roller mill.

2.2.4Desorption-resistant sediment preparation

The inoculated sediments were then desorbed immediately at the end of the five-week tumbling period using an isopropanol and electrolyte solution (0.01M NaCl, 0.01M $CaCl_2 \cdot 2H_2O$) with a ratio of 1:1(v/v) in a glass vessel. The weight ratio of sediment to the isopropanol solution was approximately 1:4.5. The vessel with sediment slurry was tumbled for 15-24 hours at the same rotation rate of sediment inoculation. At the end of desorption, the sediment slurry was centrifuged for 20 minutes in 1L plastic centrifuge bottles with relative centrifugal force of approximately 3000g and washed 3 to 4 times with electrolyte solution to remove the residual isopropanol and sodium azide. Sediment concentration and proportion of contaminant associated with reversible to desorption-resistant compartment were controlled by the number of desorption batches and the time periods of each desorption. At the end of each desorption, sediment concentrations of the model contaminants, total organic carbon content of the sediment, and sediment-water partition coefficients were measured using methods that will be described later. Tomson et al. (unpublished) has shown that desorption with this isopropanol solution allows the rapid removal of reversibly sorbed compounds, and the resulting isotherm closely tracks multiple batch-desorption in water. Isopropanol solution washing is very efficient and one-step isopropanol washing readily removes the reversibly sorbed contaminant and the remainder shows indications of desorption resistance (Lu, 2003).

2.2.5Moisture content

About 1-2 g sediment in a pre-weighed 25 ml glass vial was placed in an oven at 105 °C for 24 hours. The difference in weights represented the moisture content of the sediment

sample and was usually represented as a ratio of the moisture mass to the original weight of the wet sediment. Moisture content throughout this dissertation is presented on a wet basis.

2.2.6 Organic carbon content

Total organic carbon content (TOC) of sediment was analyzed on a Perkin Elmer 2400 series II CHN elemental analyzer (Perkin Elmer Corporation, Norwalk, CT, USA) in the Coastal Ecology Institute at LSU. First, sediment was dried at approximately 105°C overnight to remove moisture from sediment completely. Then the dried sediment was pulverized, treated with 1N HCl to remove carbonates and re-dried before it was analyzed. For each sediment sample, at least three replicates were used, and 5-15 mg sediment was taken for each replicate. The organic carbon content was usually presented as a mass fraction (f_{oc}), which is defined as the ratio of the mass of organic carbon in sediment to the total mass of dry sediment.

Before starting to measure the organic carbon content of all the contaminated sediments used in this study, organic carbon fraction of the Bayou Manchac and University Lake sediment treated with 1N HCl were compared to that of the same sediment without acidification. The measured f_{oc} of the sediment after acidification was not significantly different from the f_{oc} without acidification. This demonstrated that the inorganic carbonate fraction of the Bayou Manchac and University Lake sediment was negligible. Therefore, acidification is not necessary and organic carbon was equivalent to total organic carbon for the sediments.

Condensed phase organic carbon content of sediment was measured utilizing thermal oxidation method as stated in Gustafsson et al (1997). Operationally, organic carbon content

was measured after the sediment was combusted overnight at 375˚C with plenty of air, the fraction of oxidizable organic carbon under 375˚C was considered to be amorphous organic carbon fraction. Amorphous (f_{oc}^A) and condensed phase (f_{oc}^C) organic carbon contents of the sediment were calculated from the measured total organic carbon content of the sediment (f_{oc}) and measured organic carbon content of the sediment after combustion under 375˚C (f_{oc}^{375}) by the following two equations (2.2 & 2.3).

$$\frac{f_{oc}^{C}}{1 - f_{oc}^{A}} = f_{oc}^{375} \tag{2.2}$$

$$f_{oc}^{C} + f_{oc}^{A} = f_{oc} \tag{2.3}$$

2.2.7 Chemical analysis

Glassware used in any aspect of an experiment was cleaned thoroughly with at least 24 hours soaking in a 10% chromium acid bath. Then, the glassware was flushed with tap water, rinsed with deionized water, dried at approximately 300º C except for volumetric glassware, and stored in a clean cabinet. Volumetric glassware was dried at less than 70°C to avoid the invalidation of the calibration caused by expansion/contraction. For all solvents and chemicals, reagent grade or better quality was a basic selection criterion. The frequently used solvents such as hexane and acetone were tested once a month for purity by comparing the chromatography of the current solvent with that of the solvent before first use. Metal free deionized water from the Corning Mega-pure system was used to make all solutions.

For solid samples, ultrasonic extraction method (EPA method 3550, 1986) was used to extract PAHs from sediment matrix and a Hewlett Packard 1100 series high performance liquid chromatography (HPLC, Hewlett Packard, Palo Alto, CA, USA) with UV-Diode array

detector and fluorescence detector was used to measure the concentration of the extraction solvent (EPA method 8310, 1986). Sediment concentration of the tracers was calculated from the concentration of the extraction solvent. The extraction method used in this study was slightly modified from the EPA method and involved the following steps: 1) Weighing--Put 1 to 2g sediment samples (wet) in an extraction vessel (240ml glass jar), 2) Drying--Mix with about 20g of anhydrous sodium sulfate to dry the sediment, 3) Extraction--Add 60 ml 50/50 hexane/acetone mixture, 4) Sonicating--Sonicate for about 20 minutes in a water-bath. 5) Blow down--After sonicating, a 2 ml subsample was put into a 2 ml tube and concentrated under nitrogen flow to approximately 0.2 ml, 6) Solvent Exchanging--Add 1.8 ml acetonitrile to the tube and mix thoroughly by vortex machine. Finally, 0.5 ml to 1 ml sample after solvent exchanging was transferred to a 1.5 ml glass HPLC vial and analyzed immediately or stored in the refrigerator at 4°C for later analysis. All calculations were based on the mass balance but not on the solvent volume eliminating bias due to small solvent losses. Most results showed that the solvent loss during sonication is approximately 0.4 g, less than 1% of the total solvent used (Lu, 2003).

The concentrations of contaminants in aqueous phase were measured directly by HPLC in most measurements (EPA method 8310; SW-846 3rd edition, 1986).

2.2.8 Measurement of partition coefficient

The apparent sediment-water partition coefficients for phenanthrene were measured following the procedures of Kan et al. (1994) and standard procedures of the American Society for Testing and Materials (1998). An equivalent of 2 g wet sediment (water content of ~ 40%) was weighed per sample and placed into a 45 ml glass bottle with Teflon lined screw

cap. The bottle was then filled with electrolyte solution (0.01M NaCl, 0.01M CaCl$_2$·2H$_2$O, and 0.01 M NaN$_3$ in deionized water) with minimal headspace. At the end of the equilibration time, the sediment slurry was centrifuged at relative centrifugal force of 2000g, aqueous samples were then taken from each bottle, and the tracer concentration in water was analyzed by high performance liquid chromatography (HPLC). The tracer concentration in sediment after equilibration was calculated based on mass balance assuming that no loss of phenanthrene occurred during the experiment. Preliminary tests showed that this was a reasonable assumption as the recovery of phenanthrene was >90% after a 10-d equilibration (Lu, 2003).

2.2.9 Desorption kinetics

Amberlite XAD-2 was used as an infinite sink to desorb contaminants from sediments for the ease of controlling resulting contaminant concentration in the sediment. A certain amount of sediment, generally 100-200 grams of wet sediment, was placed in a glass jar and mixed homogeneously with 10% (mass ratio) pre-conditioned XAD-2. Preliminary studies showed that this level of XAD-2 loading was sufficient to capture all desorbed HOCs during the time frame of the experiment. The glass jar containing sediment amended with XAD-2 was sealed using aluminum foil lined screw cap and placed into an incubator keeping constant temperature at 25˚C.

XAD-2 was purchased from Supelco Inc, USA. Properties of Amberlite XAD-2 are listed in Table 2.1. XAD-2 sorbent was pre-conditioned to remove residual organics by successive washing with HPLC grade methanol and deionized water. XAD-2 resin was placed in a separatory funnel and methanol was added to maintain about one inch methanol above

XAD-2. Methanol was drained slowly after XAD-2 resin was soaked by methanol for at least one hour. Deionized water was then passed through XAD-2 resin three times to remove any residual methanol. XAD-2 was ready to use for the experiment after this pre-conditioning treatment.

Table 2.1 Properties of Amberlite XAD-2

Property	Description
Matrix	Styrene/Divinylbenzene co-polymer
Diameter	20-60 Mesh
Pore Volume	0.65 ml/g
Pore size	90 Å
Surface Area	$300m^2/g$
Density	1.08 g/ml (skeletal)
Density	1.02g/ml

At the end of the intended contact time period, sediment and XAD-2 were separated and chemical concentrations in sediment and XAD-2 resin were determined. When the sediment and XAD-2 were being separated, 100 ml of cesium chloride solution with density of 1.1 g/ml was added into 20 grams of the sediment amended with XAD-2 resin and mixed thoroughly using magnetic stirring bar. The system was then allowed to settle for 10-15 minutes until the XAD-2 was on the surface and the solution was clear enough to assure no XAD-2 stick to the interface of sediment and CsCl solution. XAD-2 was then removed via

tip-truncated glass pipette onto a sieve. The XAD-2 was then washed with tap water, and set aside to air-dry overnight. The sediment was separated from the cesium chloride solution by centrifugation at relative centrifugal force of 3000g for 20 minutes (Beckman Model J-6B Centrifuge) and washed with tap water three times to remove any residual salt. Sediment was then collected to measure chemical concentrations and moisture content.

Organic carbon content of the sediment was determined before and after XAD treatment, results showed that XAD treatment did not significantly reduce the organic carbon content of the sediment.

The beauty of using this procedure to desorb contaminants from sediments was that it limited the destruction of sediment particles to the least extent by mixing XAD2 into sediment as is without addition of water or shaking. Destruction of sediment organic matter particles often leads to over-estimating or under-estimating partition coefficients. On the other hand, it is easy to prepare enough sediment for chemical analysis and partitioning coefficient measurement.

2.2.10 Determination of fast desorption fraction of contaminants in field-contaminated sediments

Fast desorption fraction of the contaminants in sediment was determined by allowing sediment and XAD to contact for 20 hours. Experimental results on laboratory-inoculated sediment showed that the contact time of 20 hours is appropriate to characterize the fast desorption fraction of contaminants in sediments because the desorption kinetics showed that the contaminant was removed by XAD2 dramatically in the first 20 hours, then the contaminant concentration started to level off.

2.3 Results and discussion

2.3.1 Desorption kinetics in laboratory-inoculated sediments

Organic carbon contents of two lab-inoculated sediments, Bayou Manchac (BM) sediment and University Lake (UL) sediment were presented in Table 2.2. The two sediments were ideal to explore the relationship between desorption resistance and hard carbon content of the sediment in that their total organic carbon contents and soft/hard organic carbon ratio differed from each other. BM sediment had a total organic carbon content of 1.54%, 48% of which was hard organic carbon, whereas UL sediment had a total organic carbon content of 6.3%, 13% of which was hard organic carbon.

Table 2.2 Characteristics of lab-contaminated sediments

Sediment	f_{OC}	f_{OC}^{Soft}	f_{OC}^{Hard}	f_{OC}^{Soft}/f_{OC}	f_{OC}^{Hard}/f_{OC}
Bayou Manchac	1.54%	0.80%	0.74%	52%	48%
University Lake	6.3%	5.46%	0.84%	87%	13%

Desorption kinetics determined using nonpolar sorbent Amberlite XAD2 for freshly inoculated BM and UL sediment are shown in Figure. 2.1. The desorption of phenanthrene from the two sediments showed that the two sediments, with various hard carbon content, behaved almost the same. Initial concentrations of phenanthrene at the completion of inoculation were 420 and 1658 mg/Kg for Bayou Manchac and University Lake sediment respectively. Phenanthrene was removed from the sediment dramatically during the first day after XAD2 was added into sediment, then, the fraction of phenanthrene remaining in two sediments leveled off at approximated 3%.
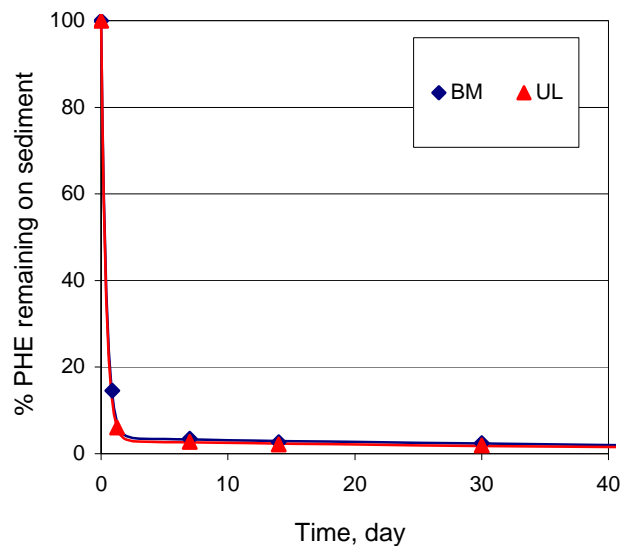
Figure 2.1 Biphasic desorption kinetics of phenanthrene from freshly inoculated BM and UL sediment. Data points were experimental data and lines were calculated from biphasic first-order model as described in Equation 1.5.

Simple empirical biphasic desorption model as described in Equation 1.5:

$$\frac{S_t}{S_0} = 1 - Fe^{-k_1t} - (1-F)e^{-k_2t}$$

was used to fit these data and gave the following parameters listed in Table 2.3. Great agreement between the model and data was observed as the R-squared value were 0.99 for both sediments. Fast desorption fractions for the two sediments were 0.96 and 0.97 respectively. This indicated that about 4% and 3% or phenanthrene in Bayou Manchac sediment and University Lake sediment were desorption resistant as determined by XAD2 desorption, showing no significant difference for the two sediments. The rate constants for fast fraction were both 0.11 h^{-1} for the two sediments, and rate constants for slow fraction were 6.1*10^{-4} and 6.6*10^{-4} respectively.

Table 2.3 Fitting parameters for desorption kinetics of phenanthrene from freshly inoculated and aged Bayou Manchac and University Lake sediments using simple empirical biphasic model

Sediment	f	k_f (h^{-1})	k_s (h^{-1})	R-squared
Fresh BM	0.964	0.108	$6.06*10^{-4}$	0.999
Aged BM	0.915	0.102	$6.14*10^{-4}$	0.998
Fresh UL	0.971	0.114	$6.58*10^{-4}$	0.999
Aged UL	0.915	0.074	$1.55*10^{-3}$	0.999

f: fast desorption fraction;
k_f: rate constant for fast fraction; k_s: rate constant for slow fraction.

Desorption kinetics determined using nonpolar sorbent Amberlite XAD2 for freshly inoculated and aged BM and UL sediment are shown in Fig. 2.2. Aged Bayou Manchac sediment had been aged for 3 years and aged University Lake sediment had been aged for 2 years. Aging effects were observed for both BM and UL sediments in Fig.2.2 because a greater fraction of phenanthrene remained in the aged sediment than the corresponding freshly inoculated sediment after desorption for 1 day which agreed with the fast desorption fraction fitted using the simple empirical model. However, no significant difference was observed for aging effects of BM and UL sediment.

The absence of difference for desorption resistance of two freshly inoculated sediments and the aging effects for the two sediments was unexpected because these two sediments showed great variation on organic matter quality. This was probably due to the very slow diffusion rate of phenanthrene in the condensed phase organic matter particles. This was reasonable because Ghosh et al (2001) utilized cryomicrotome technique and microprobe two-

step laser desorption/laser ionization mass spectrometry ($\mu L^2 MS$) to investigate the cross sectional distribution of PAHs in coal-derived and silica particles, their results suggested that most PAHs are concentrated in near external surface regions of coal-derived particles. The presumption of slow diffusion of the contaminants in coal-derived particles was supported by their modeling results because a very slow long-term release with 40% PAH remaining even after 100 years was predicted with an initial PAH concentration in the outer regions of the particle (Ghosh et al, 2001). In this context, the time length scale of the inoculation time of 5 weeks and the aging time of 2 years or 3 years were so short a time period that no significant amount of phenanthrene was migrated into the condensed phase organic matter by diffusion and thus no significant difference was observed for the desorption resistance and aging effect in the two sediments.
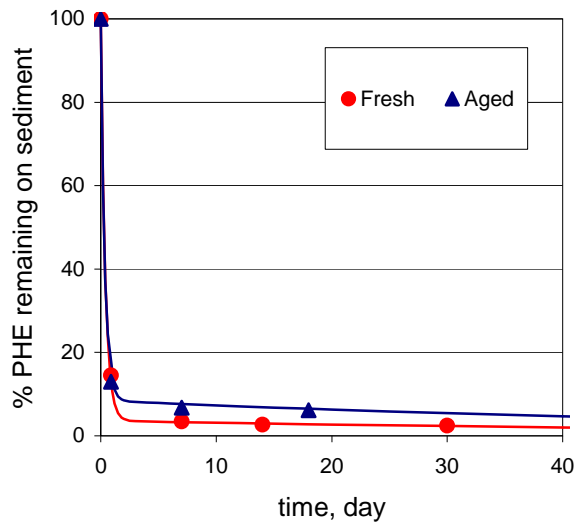
A: BM Sediment
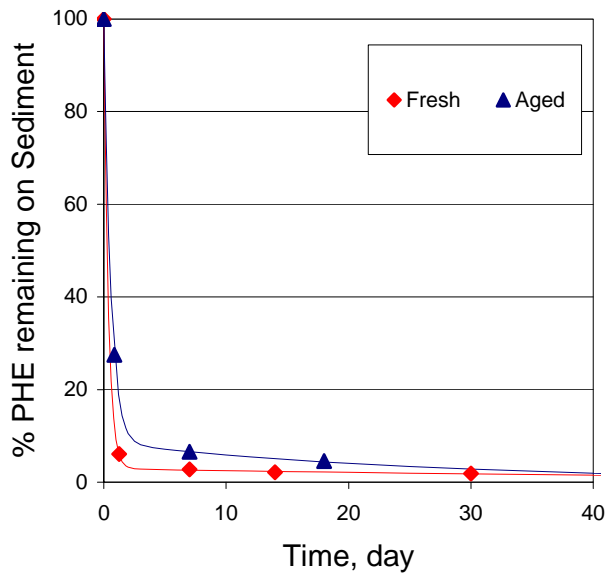
B: UL sediment

Figure 2.2 Desorption kinetics of phenanthrene from freshly inoculated and aged BM and UL sediment. Data points were experimental measurements and lines were calculated using biphasic first-order model described in Equation 1.5.

2.3.2 Desorption isotherms in laboratory-inoculated sediments

Desorption isotherms were established based on the measured initial phenanthrene concentration in sediment and aqueous phase phenanthrene concentration at the completion of the incubation for equilibration. The phenanthrene concentration in sediment at the completion of the incubation for equilibration was calculated based on the mass balance of phenanthrene. The phenanthrene concentrations in sediments were organic carbon content normalized for the ease of comparison.

The desorption isotherms of freshly inoculated BM and UL sediment are shown in Figure 2.3. Isotherms for the two sediments were almost identical. Biphasic model of Kan et al. (1998) as described in Equation 1.9:

$$q = K_{OC} \times OC \times C + \frac{K_{OC}^{irr} \times OC \times q_{max}^{irr} \times f \times C}{q_{max}^{irr} f + K_{OC}^{irr} \times OC \times C}$$

was used to fit the experimental results. The fitted maximum irreversible concentration, q_{max}^{irr}, for Bayou Manchac sediment and University Lake sediment were 6 and 25 mg/Kg respectively, these consisted of approximately 1.5% of the initial saturated phenanthrene concentrations in both sediments. The organic carbon normalized maximum irreversible concentrations in the two sediments were 430 and 440 mg/(Kg organic carbon). The results for the two sediments with different organic carbon quality showed surprising similarity that was again unexpected by the author.
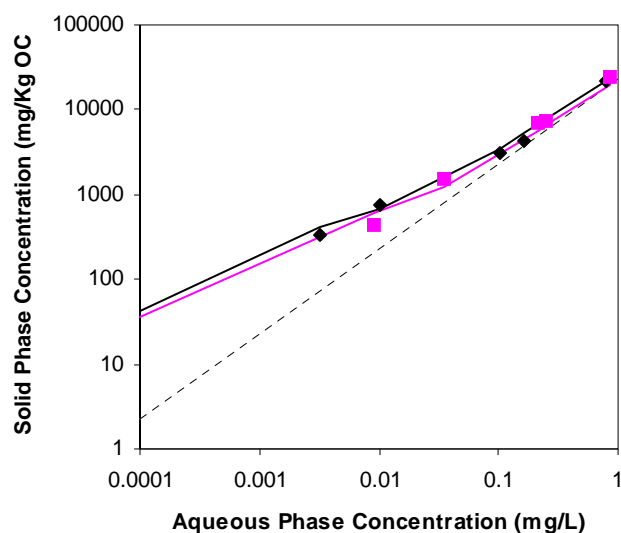
Figure 2.3 Desorption isotherm of phenanthrene in freshly inoculated Bayou Manchac and University Lake sediment. Diamonds denote BM sediment and squares denote UL sediment. Points are experimental measurements, the solid lines are the desorption isotherm of phenanthrene predicted by the biphasic model of Kan et al (1998), dashed line is the desorption isotherm predicted by reversible linear partitioning model.

The desorption isotherm of phenanthrene in freshly inoculated Bayou Manchac sediment and aged Bayou Manchac sediment were displayed in Figure 2.4 and Figure 2.5. The fitted maximum irreversible concentration, q_{max}^{irr}, for aged Bayou Manchac sediment using biphasic model of Kan et al (1998) was 20 mg/Kg and consisted of approximately 4.9% of the initial saturated phenanthrene concentrations in the sediment. The organic carbon normalized maximum irreversible concentration in the sediment was 1430 mg/(Kg organic carbon). The maximum irreversible phenanthrene concentration for aged Bayou Manchac sediment was about 3% more than freshly inoculated Bayou Manchac sediment which is correspondent to the aging effect indicated by the difference of the fast desorption fraction,

approximately 5%, measured by the desorption kinetics for freshly inoculated and aged Bayou
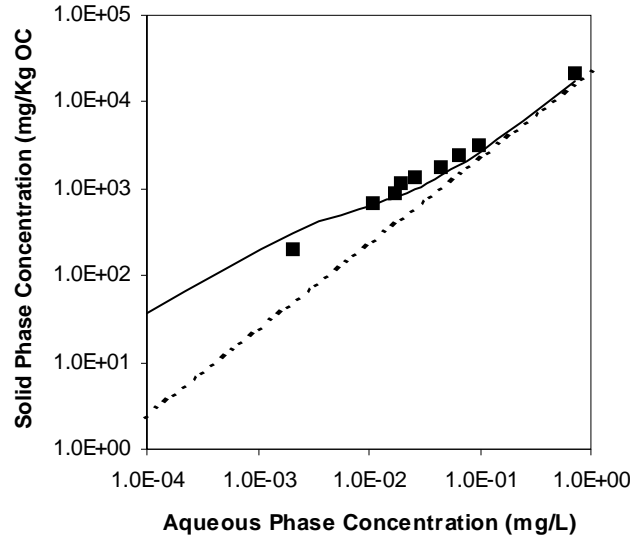
Manchac sediment.

Figure 2.4 Desorption isotherm of phenanthrene in freshly inoculated Bayou Manchac sediment. Square points are experimental measurements, the solid line is the desorption isotherm of phenanthrene predicted by the biphasic model of Kan et al (1998), dashed line is the desorption isotherm predicted by reversible linear partitioning model.
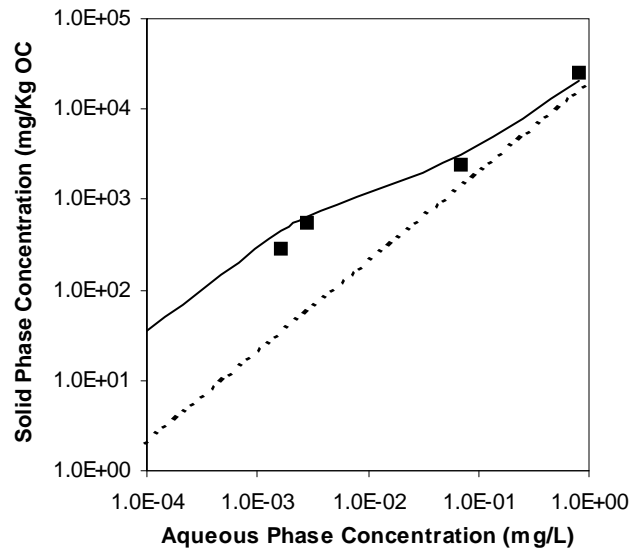
Figure 2.5 Desorption isotherm of phenanthrene in aged Bayou Manchac sediment. Square points are experimental measurements, the solid line is the desorption isotherm of phenanthrene predicted by the biphasic model of Kan et al (1998), dashed line is the desorption isotherm predicted by reversible linear partitioning model. Sediment was aged for 3 years.

2.3.3Effect of equilibration time on the apparent equilibrium

To evaluate the possibility of the experimental artifacts from a shortened equilibration time acting as the primary reason to the desorption hysteresis of hydrophobic organic contaminants indicated by the desorption isotherm, the apparent desorption isotherms of phenanthrene in freshly inoculated Bayou Manchac sediment determined at equilibration time of 10 days and 60 days are shown in Figure 2.6 and corresponding apparent partition coefficients are presented in Table 2.4. The equilibration time of 10 days was elucidated because desorption isotherms were determined by many researchers at comparable time length scale. For instance, Kan et al (1998) determined desorption isotherms at 1-3 days, Huang and Weber (1997a) measured desorption isotherms at 14 days. Longer equilibration time of 60 days was used to investigate the potential effect of extended equilibration time on the apparent partition coefficient.
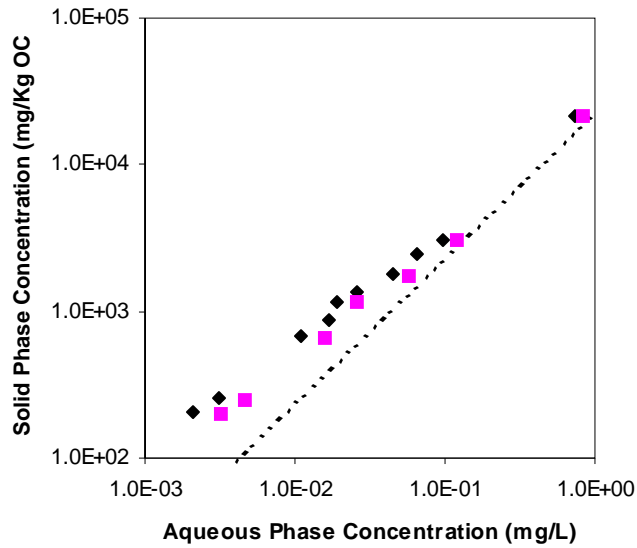
Figure 2.6 Apparent desorption isotherms of phenanthrene in freshly inoculated Bayou Manchac sediment at different equilibration time. Diamonds denote measurements obtained at equilibration time of 10 days and squares 60 days. Dashed line is the desorption isotherm predicted by reversible linear partitioning model.

The apparent organic carbon normalized partition coefficient of phenanthrene in Bayou Manchac sediments with different desorption-resistant phenanthrene concentration in Table 2.4 suggested that prolonged equilibration time results in a less partition coefficient. The difference ranged from 0.07 to 0.20 logarithmic unit. Interestingly, the difference increased as the phenanthrene concentration in the sediment became lower and lower. These observations were reasonable because the desorption-resistant phenanthrene in hard carbon became to be the dominant contaminant in the sediment which controlled its release into aqueous phase. On the other hand, biphasic model of Kan et al (1998) was used to fit the desorption isotherm determined at 60 days, however, the model predicted curve did not offer good agreement with the experimental data. This was not surprising because the model of Kan et al (1998) was developed based on their desorption isotherms determined using equilibration

time of 1-3 days. These findings were consistent with Huang and Weber (1997) that apparent

equilibria obtained by relatively geologically old materials within 28 days did not approach

real stable state.

Table 2.4 Apparent partition coefficients of phenanthrene in Bayou Manchac sediments with
different desorption-resistant phenanthrene concentrations determined at 10days and 60days

Sediment Loading	LogKoc, app At 10 days	LogKoc,app At 60 days	Difference
380.33±10.09	4.47±0.002	4.40±0.01	0.07
49.99±1.73	4.51±0.002	4.41±0.01	0.10
38.97±0.27	4.59±0.01		
29.59±0.61	4.63±0.02	4.50±0.01	0.13
20.94±1.09	4.73±0.01		
17.51±0.27	4.78±0.005	4.64±0.03	0.14
13.39±0.78	4.72±0.01		
10.16±0.14	4.79±0.01	4.62±0.02	0.17
3.81±0.14	4.92±0.02	4.74±0.02	0.18
2.99±0.01	4.99±0.03	4.79±0.03	0.20

The above results indicated that the desorption resistance represented by the deviation

of desorption curve from the projected adsorption line on desorption isotherms might not be

real desorption resistance if long enough equilibration time were waited for the system to

reach true equilibria.

2.3.4Fast desorption fraction in field contaminated sediments

The fast desorption fraction F, was operationally defined by the equation 2.4,

$$F = \frac{(C_0 - C_{Des20hr})}{C_0} \qquad (2.4)$$

where C_0 was the initial concentration of contaminant in sediment and $C_{Des20hr}$ was the concentration of contaminant in sediment after treatment with XAD2 for 20 hours. The proportion of contaminants removed by XAD2 in the first 20hours was considered to be the fast desorption fraction or called labile fraction while the proportion of contaminants remaining in sediment after XAD2 treatment for 20 hours was considered to be desorption resistant fraction in the sediment.

Fast desorption fractions of contaminants in Utica harbor and Rouge River sediment were presented in Table 2.5 and 2.6. The fast desorption fraction of a number of PAHs ranged from 0.12 to 0.46 in Utica Harbor sediment and from 0.21 to 0.44 in Rouge River sediment. As expected, the fast desorption fraction in Rouge River sediment for different compound generally decreased as the molecular size increased because of the steric hindrance effect. But this trend was not observed in Utica Harbor sediment and it was not clear what was the reason leading to the absence of the trend observed in Rouge River sediment. The average of fast desorption fraction for all compounds in Utica Harbor and Rouge River sediment were 0.28 and 0.35 respectively. Note that the fraction of condensed phase carbon in the total organic carbon in the two sediments were 39% and 25% as shown in Table 2.7, which indicate that the averages of fast desorption of the compound of interest correlated inversely to the condensed phase carbon contents of the two sediments. These observations revealed that the

desorption resistant fraction as determined by XAD2 treatment were well connected to the condensed phase carbon content as defined by the combustion method at 375°C.

Table 2.5 Fast desorption fractions of contaminants in Utica Harbor sediment

Compound	C_0^a (mg/Kg)	$C_{Des20hr}^b$ (mg/Kg)	F^c
Phe	6.5(±0.22)	5.1(±0.12)	0.22
Ant	5.8(±0.10)	4.2(±0.14)	0.28
Pyr	23.8(±0.45)	18(±0.34)	0.24
Chr	24.1(±1.03)	17.2(±0.75)	0.29
BbF	8.9(±0.31)	4.8(±0.19)	0.46
BkF	4.2(±0.05)	3.7(±0.06)	0.12
BaP	12.7(±0.36)	9.3(±0.33)	0.27
DBahA	7.6(±0.08)	5.9(±0.14)	0.22
BghiPe	5.4(±0.21)	3.2(±0.15)	0.41

a: C_0: Initial concentrations of contaminants in sediment
b: $C_{Des20hr}$: Concentrations of contaminants in sediment after treatment with XAD2 for 20 hours
c: F is fast desorption fraction, operationally defined by the $(C_0-C_{Des20hr})/C_0$

Table 2.6 Fast desorption fractions of contaminants in Rouge River sediment

Compound	C_0^a (mg/Kg)	$C_{Des20hr}^b$ (mg/Kg)	F^c
Phe	22.9(±0.48)	12.8(±0.19)	0.44
Ant	8.1(±0.23)	4.5(±0.17)	0.44
Pyr	36.5(±1.25)	24.7(±0.88)	0.32

Chr	22.4(±1.01)	13.9(±0.32)	0.38
BbF	15.4(±0.54)	9.5(±0.29)	0.38
BkF	8.8(±0.37)	5.6(±0.16)	0.36
BaP	11.6(±0.28)	8.8(±0.35)	0.24
DBahA	21.2(±0.46)	16.7(±0.53)	0.21
BghiPe	14.5(±0.32)	9.7(±0.14)	0.33

a: C_0: Initial concentrations of contaminants in sediment

b: $C_{Des20hr}$: Concentrations of contaminants in sediment after treatment with XAD2 for 20 hours

c: F is fast desorption fraction, operationally defined by the $(C_0-C_{Des20hr})/C_0$

Table 2.7 Characteristics of field-contaminated sediments

Sediments	f_{OC}*	f_{OC}^A	f_{OC}^C	f_{OC}^A/f_{OC}	f_{OC}^C/f_{OC}
Utica Harbor	2.1%	1.28%	0.82%	61%	39%
Rouge River	7.9%	5.93%	1.98%	75%	25%

*Data was obtained after the sediments sieved through 2mm sieve;

F_{OC}^A: amorphous organic carbon content;

f_{OC}^C: Condensed phase organic carbon content.

2.3.5 Partition coefficients of contaminants in bulk sediment and resistant fraction in field contaminated sediments

Apparent partition coefficients of contaminants in bulk sediment, resistant fraction measured in Utica Harbor and Rouge River sediment were presented in Table 2.8 and 2.9.

The resistant fraction was the fraction of contaminants remaining in the sediments after the sediments were treated using XAD2 for 20 hours. The literature data of logarithm of organic carbon normalized partition coefficient was calculated from LogKow values compiled by Mackay et al. (1991) using the correlation reported by Karickhoff *et al.* (1979) as equation 2.5.

$$LogK_{OC} = 1.0 * LogK_{OW} - 0.21 \qquad (2.5)$$

The organic carbon normalized apparent partition coefficient for contaminants in bulk sediment and for the resistant fraction in sediments were measured at the equilibration time of 10 days. The logarithm of organic carbon normalized apparent partition coefficient for labile fraction contaminants in sediment was calculated assuming the contaminants in aqueous phase when measuring apparent partition coefficient in bulk sediment was released by available fraction or called fast desorption fraction only. Thus, for an individual compound, the logarithm of organic carbon normalized apparent partition coefficient for labile fraction contaminants was correlated with fast desorption fraction F and the logarithm of organic carbon normalized apparent partition coefficient for contaminants in bulk sediment according to equation 5.3,

$$LogK_{OC}{}^{Labile} = LogK_{OC}{}^{Bulk} + LogF \qquad (2.6)$$

As shown in Table 2.8 for Utica Harbor sediment, the apparent partition coefficient of a certain contaminant in desorption resistant fraction was significantly greater than that in bulk sediment which was also significantly greater than the corresponding literature value. Interestingly, the apparent partition coefficients all contaminants in labile fraction were

comparable to those theoretical values from literature. These observations suggested that the labile fraction of the contaminants associated with sediment controlled the short-term release.

Table 2.8 Apparent partition coefficients for bulk Utica Harbor sediment, resistant fractions and labile fractions in Utica Harbor sediment

Compound	Log K_{OC}, Literature[a]	Log K_{OC},app Bulk	Log K_{OC},app Resistant	Log K_{OC}, Labile[b]
Phe	4.36	4.78	4.99	4.12
Ant	4.33	4.96	5.12	4.40
Pyr	4.97	5.40	5.97	4.79
Chr	5.65	6.32	6.73	5.77
BbF	5.59	6.58	-	6.25
BkF	5.79	6.65	7.17	5.72
BaP	5.83	6.70	7.28	6.13

a: Log Koc in literature was calculated from LogKow compiled in Mackay et al. 1991 using correlation reported Karickhoff *et al*. 1979 (LogKoc = 1.0 * LogKow – 0.21).

b: LogKoc for labile fraction was calculated assuming the concentration in water for bulk sediment was contributed by available fraction only

Comparing the Utica Harbor sediment with Rouge River sediment, similar results were also obtained for Rouge River sediment. Generally, for bulk sediment, the apparent partition coefficients of smaller size molecules like PHE, ANT and PYR were almost identical for the two sediments, while the apparent partition coefficients of larger size molecules like CHR, BbF, BkF and BaP in Rouge River sediment were significantly less than

those in Utica Harbor sediment. The apparent partition coefficients of all compounds in desorption resistant fraction in Rouge River sediment were less than those in Utica Harbor sediment. No clear interconnection between apparent partition coefficients of contaminants in these two sediments and their corresponding condensed phase organic carbon contents were observed because the apparent partition coefficient measured in this study were measured in a very short term period, which was 10 days. The possible potential correlation was probably masked by the extremely slow kinetic effect of the contaminants migrating in the condensed phase organic carbon.

Table 2.9 Apparent partition coefficients for bulk Rouge River sediment, resistant fractions and labile fractions in Rouge River sediment

Compound	Log K_{OC}, Literature[a]	Log K_{OC},app Bulk	Log K_{OC},app Resistant	Log K_{OC}, Labile[b]
Phe	4.36	4.87	4.91	4.52
Ant	4.33	4.84	5.06	4.49
Pyr	4.97	5.43	5.64	4.94
Chr	5.65	6.03	5.99	5.62
BbF	5.59	6.21	6.30	5.79
BkF	5.79	6.31	-	5.86
BaP	5.83	6.34	6.86	5.86

a: Log Koc in literature was calculated from LogKow compiled in Mackay et al. 1991 using correlation reported Karickhoff *et al*. 1979 (LogKoc = 1.0 * LogKow – 0.21).

b: LogKoc for labile fraction was calculated assuming the concentration in water for bulk sediment was contributed by available fraction only

2.4Summary

Desorption resistance for BM and UL sediments were not significantly different, though the two sediments have different soft and hard carbon contents. About 3 and 4% of the original saturated phenanthrene in BM and UL sediment were considered to be slow desorption fraction of desorption-resistant fraction according to the desorption kinetics determined using XAD2 nonpolar sorbent. These were comparable to the maximum irreversible concentration, q_{max}^{irr}, determined by fitting desorption isotherms using Kan et al's biphasic sorption/desorption model, which indicated that about 1.5% of the original saturated phenanthrene was desorption-resistant fraction. Aged sediment exhibited greater desorption resistance for both BM and UL sediment. Again no significant deviation on aging effects was observed for BM and UL sediments.

The absence of correlation between desorption resistance and condensed phase organic carbon content in laboratory-inoculated BM and UL sediment was most likely due to the extremely slow diffusion rate of contaminant in condensed phase organic carbon. The time scale of 5 weeks for inoculation and two to three years of aging period were not long enough for a considerable amount of contaminant to migrate into the condensed phase organic carbon.

Prolonged equilibration time for Bayou Manchac sediment exhibited less apparent partition coefficients. Different apparent partition coefficients with different equilibration time reflected that the slow diffusion of the contaminants into the hard carbon particles is most likely the cause to the result. The desorption resistance represented by the deviation of desorption curve from the projected adsorption line on desorption isotherms might not be real

desorption resistance if long enough equilibration time were waited for the system to reach true equilibria.

Fast desorption fraction of the same contaminant in different sediments varied a lot because of different sediment properties. Utica Harbor sediment, with higher condensed phase carbon content, exhibited lower fast desorption fraction than Rouge River sediment with lower condensed phase carbon content. The desorption resistant fractions as determined by XAD2 treatment for field-contaminated sediments were well connected to the condensed phase carbon content as defined by the combustion method at 375°C, greater condensed phase carbon content indicating less fast desorption fraction.

Organic carbon normalized apparent partition coefficient for bulk sediment, resistant fraction and available fractions showed that only fast desorption fraction or called labile fraction of contaminants was available for short term equilibrium partitioning.

In order to understand clearly the underlying reason for the desorption resistance, size and density separation might be helpful to figure out what fraction of the sediment contribute mostly to the desorption resistance.

CHAPTER 3 SIZE AND DENSITY SEPARATION

3.1 Introduction

Desorption resistance of HOCs in sediment has been widely ascribed to the heterogeneity of organic matter in sediments and soils. Condensed phase organic carbon has been considered to be responsible for the sequestration of HOCs in sediments while amorphous natural organic matter has been thought to exhibit no desorption resistance.

Some researchers has conducted experiments to fractionate sediment into different fractions to understand the desorption resistance behavior (Rockne et al., 2002; Ghosh et al., 2000; Ghosh et al., 2001). However, no effort has been put to separate clearly the amorphous natural organic matter and condense phase organic matter from sediment. This chapter was focused on size and density separation of the sediments with the objective of isolating the amorphous and condensed phase organic carbon completely and understanding the availability of HOCs in each category of organic matter. Contaminant distribution and sediment mass distribution in various sediment fractions as well as the availability of contaminant in each fraction were discussed.

3.2 Materials and Methods

3.2.1 Sediments

Bayou Manchac sediment was used for this study. The desorption-resistant sediments were prepared using the procedures described in chapter 2 after the sediment was inoculated with phenanthrene. The resulting series of Bayou Manchac sediments in Chapter 2 after

different number of isopropanol/water solution washing steps and time that contained different phenanthrene concentrations were used for this study.

3.2.2 Separation of sediments

Separation of sediments using wet sieving and high-density solution were similar to the procedures described by Mayer et al. (1993) and Ghosh et al. (2000) with minor modification. One hundred grams of wet sediment was added into a 500ml glass jar, 200ml of water was added into the jar and mixed thoroughly using spatula. After the system settled on bench top for three minutes, the light material floating in the water were collected and passed through a series of sieves (63μm, 150μm, 250μm). This step was repeated until the water became not cloudy. Then 100 ml CsCl (Purchased from Fisher Scientific) solution with a specific gravity of 1.8 was added into the jar and mixed completely. After the system settled on bench top for three minutes, the light material floating in the CsCl solution together with CsCl solution were collected and passed through the above mentioned series of sieves. By now sediment was separated into five fractions including one heavy fraction left in the glass jar mostly consisting of sand, three light fractions on the sieves, and one last light fraction which is less than 63μm in size with plenty of water and CsCl solution. The first four fractions were rinsed with water to completely remove residual CsCl. The light fraction less than 63μm in size was centrifuged at relative centrifugal force of 2000g for 20 minutes and washed with water 3 times to make sure there is no CsCl remaining in this fraction. The heavy fraction was sieved using 63μm sieve to split it into two fractions.

Thus, the sediment was separated into six fractions, four light fractions which are <63μm L, 63~150μm L, 150~250μm L, >250μm L and two heavy fractions which are <63μm H and >63μm H. Fraction <63μm L consist of mostly clay and silt and organic matter,

fractions 63~150μm L, 150~250μm L, and >250μm L consist of mainly organic matter, and fractions <63μm H and >63μm H mainly sand.

The mass of each fraction was measured after each fraction was air-dried at the completion of fractionation of the sediment. Contaminant concentrations and availability indicated by apparent partition coefficient in different size and density fractions were analyzed following the procedures for solid samples stated in chapter 2. Apparent partition coefficient of contaminant in each fraction was measured according to the procedure stated in chapter 2.

3.3 Results and Discussion

3.3.1 Contaminant distribution in different fractions

Separation experiments were conducted with the original intention to separate soft carbon and hard carbon from the sediment of interest to characterize these two categories of carbonic matter separately, preliminary results, however, showed that it was impossible to fulfill the proposed objective. Therefore, the sediment was fractionated in the way stated in section 3.2.2 to investigate the distribution and corresponding availability of phenanthrene in resulting six fractions which are four light fractions, <63μm L, 63~150μm L, 150~250μm L, >250μm L and two heavy fractions, <63μm H and >63μm H.

Bayou Manchac sediments prepared in chapter 2 with different concentrations of desorption-resistant phenanthrene as presented in Table 3.1 were used for the separation experiment. Each sediment was fractionated into the above stated six fractions. Sediment material balance and phenanthrene balance in each of these five sediments ranged from 0.97 to 0.99 and from 0.98 to 1.09 respectively.

Table 3.1 Bayou Manchac sediments with different concentrations of desorption-resistant phenanthrene prepared by stepwise isopropanol solution batch wash

Sediment	Level I	Level II	Level III	Level IV	Level V
Loading (mg/Kg)	49.99±1.73	38.97±0.27	13.39±0.78	10.16±0.14	3.81±0.14

Sediment mass and phenanthrene concentration in each fraction and percentage of phenanthrene in each fraction out of total phenanthrene in the sediment used for fractionation were displayed in Figure 3.1 to 3.5 where top figure presents the sediment mass distribution in each fraction, middle one presents phenanthrene concentration in each fraction and bottom one presents phenanthrene percentage in each fraction out of the total phenanthrene in the whole sediment for separation.

Fraction <63μm L consist of mostly clay and silt and organic matter, fractions 63~150μm L, 150~250μm L, and >250μm L consist of mainly organic matter, and fractions <63μm H and >63μm H mainly sand. It suggested in Table 3.2 that phenanthrene concentration in fractions mostly consist of organic matter (63~150μm L, 150~250μm L, and >250μm L) were close to each other and were significantly higher than in fractions rich in inorganic material. Phenanthrene concentrations in these three fractions were up to 18 times higher than the corresponding whole sediment loading. Phenanthrene concentration in light fraction <63μm L which is mainly clay and silt and organic matter was in the same order of magnitude as in the corresponding whole sediment. Phenanthrene concentration in heavy fractions were much less than in corresponding whole sediment.

Table 3.2 Phenanthrene concentration (mg/Kg) for fractionated Bayou Manchac sediment with different concentrations of desorption-resistant phenanthrene

Sediment	Sediment Loading	<63μm L	63-150μm L	150-250μm L	>250μm L	Heavy
Level I	49.99±1.73	74.44±2.35	754.68±15.82	422.32±17.35	892.7±3.57	9.63±0.47
Level II	38.97±0.27	54.05±1.57	630.76±28.39	451.03±21.94	547.86±16.89	3.97±0.24
Level III	13.39±0.78	18.45±0.05	86.07±4.71	86.02±3.74	165.20±26.56	2.16±0.21
Level IV	10.16±0.14	18.91±0.70	49.64±2.64	42.50±0.58	145.10±3.19	1.69±0.11
Level V	3.81±0.14	7.46±0.02	43.10±2.19	8.55±0.26	30.14±1.35	0.61±0.03

As far as the material balance of sediment and phenanthrene in the sediment is concerned, three light fractions rich in organic matter (63~150μm L, 150~250μm L, and >250μm L) consist of about three percent of the sediment mass, but the sum of phenanthrene amount in these fractions consist of 17 to 36 percent of total phenanthrene in the corresponding whole sediment. Taking light fraction <63μm L into account, the phenanthrene in all these four fractions consist about 90 percent of the total phenanthrene in the corresponding whole sediment.

These findings were consistent with the observations reported by Ghosh et al. (2000) that the coal/wood-derived particles constitute only 5% of the sediment by weight but contain 62% of the total PAHs, and by Rockne et al. (2002) that 50-80% PAHs were associated with the low density fraction which represents only 3-15% of total sediment mass in the two sediments they studied. These observations were not surprising because hydrophobic organic contaminants were expected to be mainly associated with organic matter in sediments.
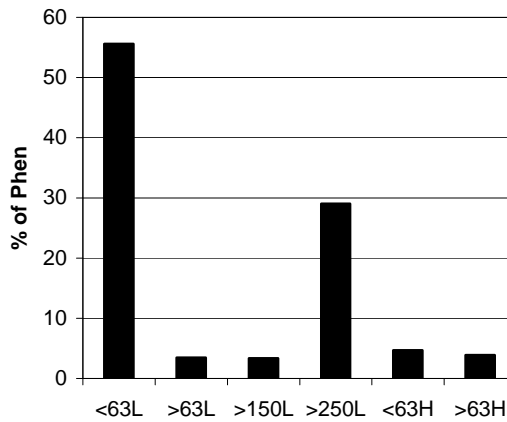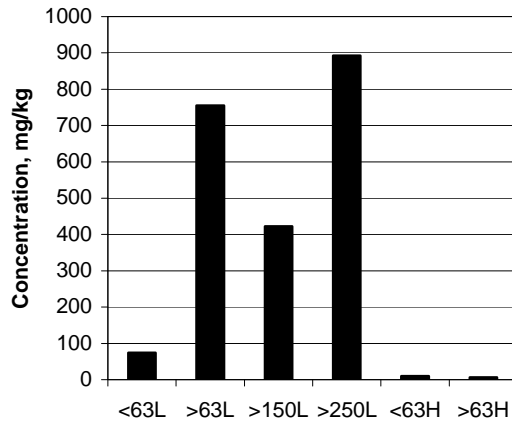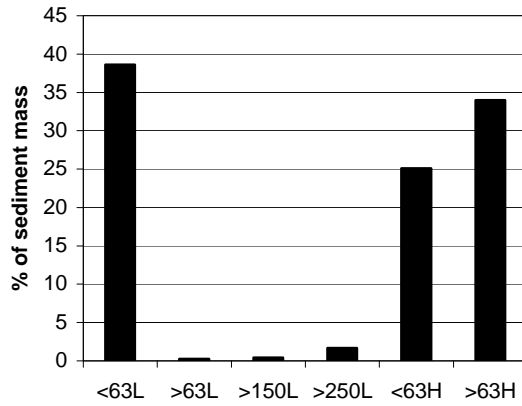
Figure 3.1 Phenanthrene distribution in fractionated Bayou Manchac sediment Level I (50 mg/Kg). Top figure is the sediment mass distribution in each fraction, middle one is phenanthrene concentration in each fraction and bottom one is phenanthrene percentage in each fraction out of the total phenanthrene in the whole sediment for separation.
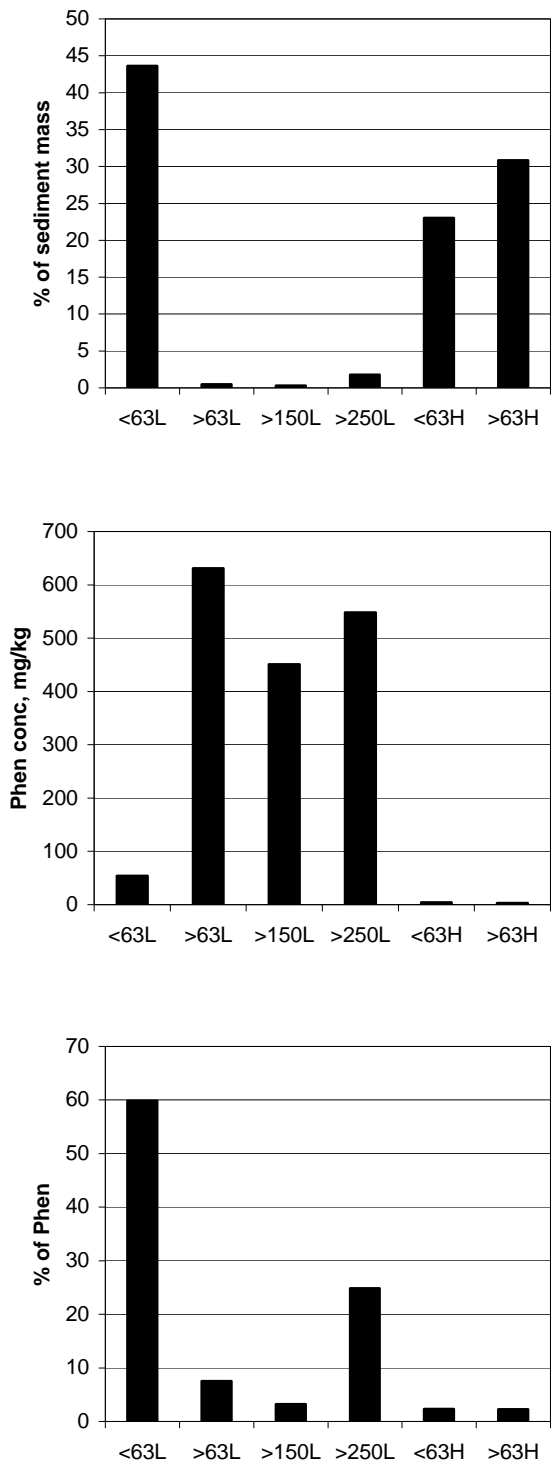
Figure 3.2 Phenanthrene distribution in fractionated Bayou Manchac sediment Level II (39 mg/Kg).
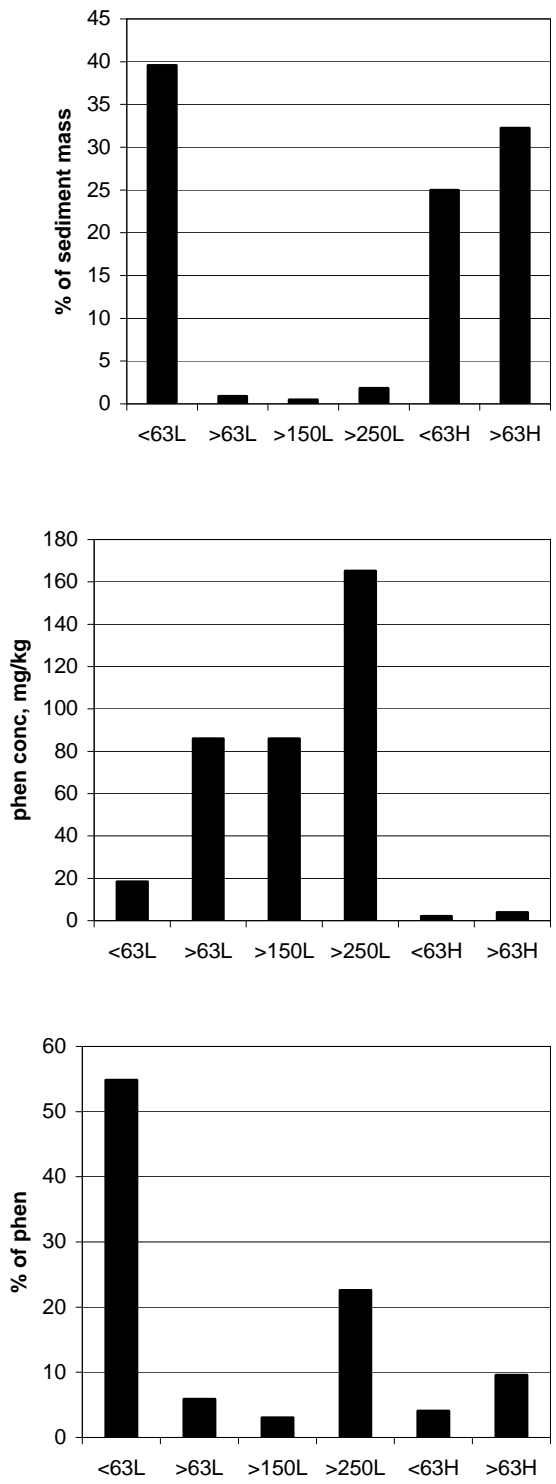
Figure 3.3 Phenanthrene distribution in fractionated Bayou Manchac sediment Level III (13.4 mg/Kg).
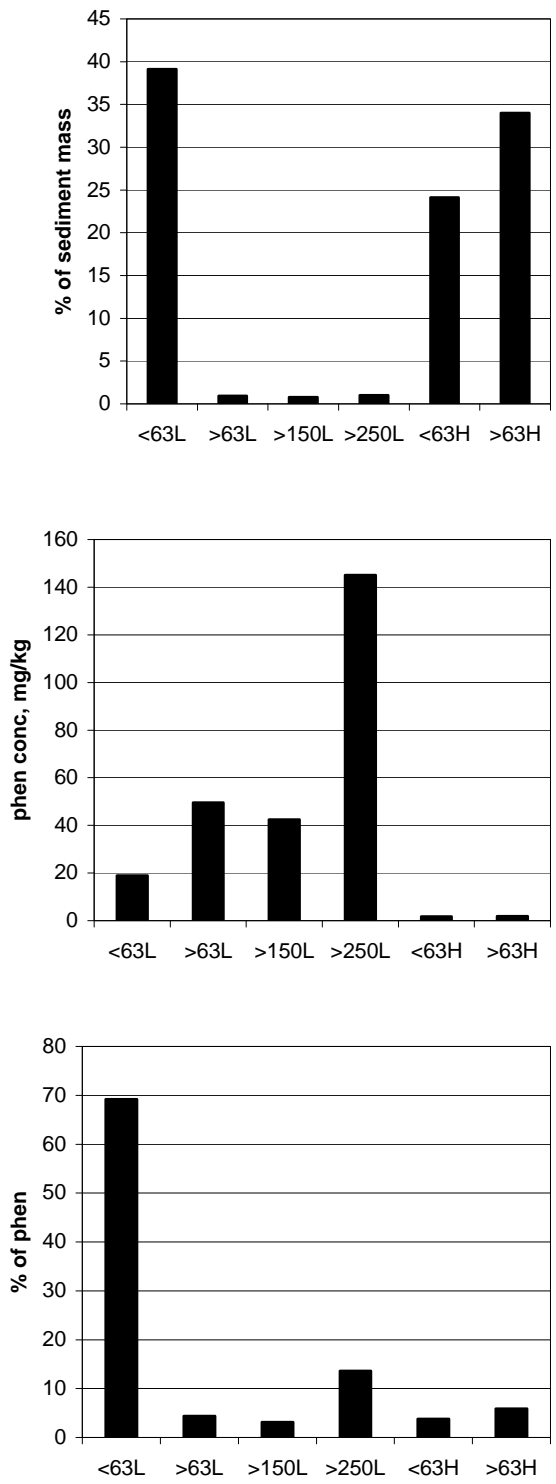
Figure 3.4 Phenanthrene distribution in fractionated Bayou Manchac sediment Level IV (10.2 mg/Kg).
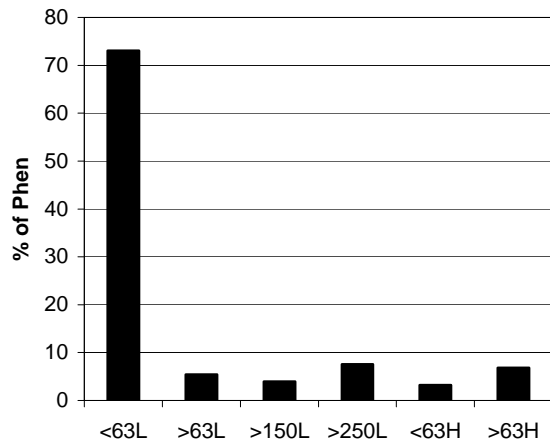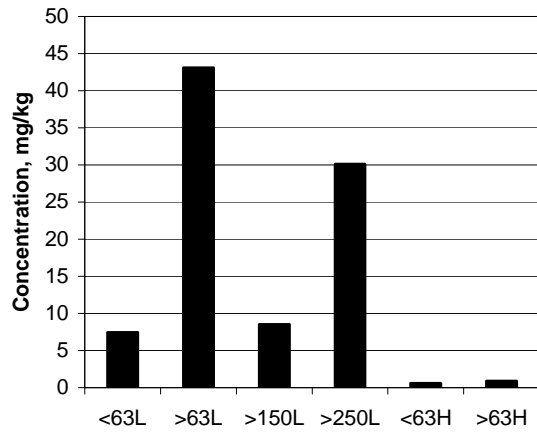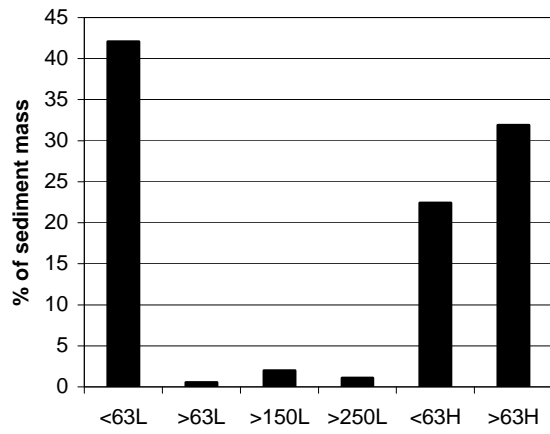
Figure 3.5 Phenanthrene distribution in fractionated Bayou Manchac sediment Level V (3.81 mg/Kg).

3.3.2 Apparent partition coefficients of contaminants in sediment fractions

To evaluate the availability of the contaminants in fractionated sediments, organic carbon content and apparent partition coefficients of phenanthrene in fractionated sediments were determined. Table 3.3 showed the apparent organic carbon normalized partition coefficients of phenanthrene in fractionated Bayou Manchac sediments with different concentrations of desorption-resistant phenanthrene.

Table 3.3 Apparent partition coefficients (Log Koc) for fractionated Bayou Manchac sediment with different concentrations of desorption-resistant phenanthrene

Sediment	Whole sediment	<63µm L	63-150µm L	150-250µm L	>250µm L	Heavy
Level I	4.51±0.01	4.60±0.02	4.60±0.02	4.47±0.03	4.67±0.01	4.60±0.02
Level II	4.59±0.01	4.64±0.01	4.74±0.03	4.60±0.03	4.64±0.02	4.40±0.02
Level III	4.72±0.01	4.88±0.03	4.51±0.02	4.52±0.02	4.84±0.02	4.90±0.02
Level IV	4.79±0.01	5.05±0.02	4.47±0.02	4.48±0.01	4.99±0.03	4.89±0.03
Level V	4.92±0.02	5.02±0.02	4.95±0.03	4.57±0.03	4.90±0.02	4.83±0.03

* f_{oc}'s were 1.95% for fractions <63µm L, with condensed phase carbon content/f_{oc} of 49%;
** f_{oc}'s were 18.81% for fractions 63-150µm L, 150-250µm L and >250µm L, with condensed phase carbon content/f_{oc} of 46%;
*** f_{oc}'s were 0.40% for Heavy fraction respectively.

The logarithm of apparent organic carbon normalized partition coefficients for whole sediments with different concentration of desorption-resistant phenanthrene ranged from 4.51 to 4.99 and it increased as the phenanthrene concentration in whole sediment decreased because the desorption-resistant phenanthrene represented larger and larger fraction in the

sediment when reversibly sorbed phenanthrene was washed away by increasing wash steps and extended washing time. The logarithm of organic carbon normalized apparent partition coefficients of phenanthrene in sediment fractions also followed this trend. However, no trend or significant difference was observed between fractions separated from a single whole sediment. This suggested that separation of sediment did not give us much information regarding in which fraction the desorption-resistant phenanthrene was sequestered and availability of sequestered phenanthrene. One major hindrance resulting in this situation was that the fractionation of sediment did not give us a clear-cut separation of amorphous and condensed phase carbon from the sediment.

3.4 Summary

Phenanthrene concentration in light fractions rich in organic matter were significantly greater than in light fraction rich in clay and silt and than in heavy fractions rich in sand.

Availability of phenanthrene in fractionated sediment indicated by the apparent partition coefficients showed no significant difference for different fractions. Thus, size and density separation does not help to understand the desorption resistance of HOCs in contaminated sediments due to the absence of ease to separated amorphous and condensed phase organic carbon completely from the sediment.

CHAPTER 4 COARSE PARTICLES IN FIELD CONTAMINATED SEDIMENTS

4.1 Introduction

As stated in Chapter 3, detailed size and density separation did not provide much information helpful to understand sequestration of HOCs in sediment in that it is impossible to have a clear-cut separation of different category of organic matter in sediment. It is, however, easy to differentiate coarse particles visually. Enough material could be obtained with ease to perform chemical analysis and other particle characterization.

This chapter focused on the characterization of coarse particles as a practical way to investigate the desorption resistance of HOCs in sediments.

4.2 Materials and Methods

4.2.1 Sediments

Two field-contaminated sediments (Utica Harbor sediments, Rouge River sediment) were used in this research. Utica Harbor sediment was collected from Utica Harbor, NY. It was not sieved when received. Rouge River sediment was collected from Rouge River, MI. Rouge River sediment had been sieved through 2 mm sieves when received.

4.2.2 Obtaining coarse particles from sediments

Generally, coal/coal-derived particles, woody/wood-derived particles, soot particles and other particles high in organic carbon content have been considered to be responsible for the sequestration of HOCs in sediment.

Utica Harbor sediment was passed through 2mm sieve since it had not been sieved before it was received. Rouge River sediment was passed through 400 μm to obtain enough

coarse particles note that this sediment had been passed through 2mm sieve before it was received. Coarse particles were air-dried at room temperature.

Different categories of coarse particles were selected manually from those particles remaining on the sieve. Four main categories of particles were collected and they were denoted as coal-like, coal cinder, woody and charcoal. Coal-like particles were visibly black, nonporous and shiny particles. Coal cinder particles were gray black and porous particles. Woody particles were cellulosic particles looking like trunk segment. Charcoal particles were burned cellulosic and porous particles.

4.2.3 Particle characterization

Major PAHs concentrations monitored are listed in Table 4.2.

Table 4.1 Major PAHs of interest and selected properties

Compound	Log K_{OW}[a]	Log K_{OC}[b]	Molecular Weight
Phe	4.57	4.36	178
Ant	4.54	4.33	178
Pyr	5.18	4.97	202
Chr	5.86	5.65	228
BbF	5.80	5.59	252
BkF	6.00	5.79	252
BaP	6.04	5.83	252
DBahA	6.5	6.29	278
BghiPe	6.75	6.54	276

a. Mackay et al. 1991, Illustrated Handbook of Physical-Chemical Properties and Environmental Fate for Organic Chemicals, Vol. II, Polynuclear Aromatic Hydrocarbons, Polychlorinated Dioxins, and Dibenzofurans;

b. Calculated from LogKow using correlation reported Karickhoff *et al.* 1979 (LogKoc=1.0*LogKow–0.21).

Contaminant concentrations were determined directly in coarse particles from Rouge River sediment following the procedures for solid samples stated in Chapter 2. The coarse particles from Utica sediment was ground and passed through 2mm sieve to make sure the they possessed similar particle size as sediments used in the study. Total organic carbon content, amorphous and condensed phase organic carbon contents were measured for these particles. Apparent partition coefficients of contaminants were also measured in order to examine sequestration of contaminants in different categories of particles.

4.2.4 Sorption of phenanthrene to different particles

To test the ability and rate of sorption of phenanthrene to different types of coarse particles, coal-like, coal cinder, wood and charcoal particles were used to conduct the sorption experiment. Phenanthrene aqueous solution was added to each glass jar containing pre-weighed coarse particles, aqueous phenanthrene concentration was monitored by the end of sorption experiment.

4.2.5 pH effect on availability of PAHs in coarse particles

Apparent partition coefficients for a variety of PAHs on those coarse particles were determined under different pH values to evaluate the effect of pH value on the availability of PAHs. Buffer solution with different pH values were used to substitute electrolyte solution in the measurement of apparent partition coefficient stated in Chapter 2.

4.3 Results and Discussion

4.3.1 Characterization of different coarse particles

Organic carbon contents of different particles with high organic carbon contents from Utica sediment were determined and presented in Table 4.2. Organic carbon contents of these particles ranged from 28.8% to 83.1%. These observations were comparable to organic carbon contents reported in Jonker and Koelmans (2002) for coal-like of 90.8%, coal soot of 32.2% and charcoal of 82.2%. The amorphous and condensed phase organic carbon contents, however, were different from observations by Jonker and Koelmans. This could be ascribed to different places where these sediments were collected.

Table 4.2 Organic carbon content of different particles from Utica sediment

Particles	f_{OC}	f_{OC}^{Soft}	f_{OC}^{Hard}	f_{OC}^{Soft}/f_{oc}	f_{OC}^{Hard}/f_{OC}
Coal-like	80.9%	39.4%	41.5%	48.7%	51.3%
Coal cinder	28.8%	7.4%	21.4%	25.7%	74.3%
Wood	56.0%	56.0%	0%	100%	0%
Wood charcoal	83.1%	82.7%	0.4%	99.5%	0.5%

Concentrations of contaminants in coarse particles from Utica harbor, Rouge River and Indiana Harbor sediment and concentrations of contaminants in corresponding whole sediment are listed in Table 4.3 and 4.4 respectively. Although chemical analysis of coarse particles in these sediments showed high variation in concentrations of PAHs as indicated by total PAHs concentration up to 2,735 mg/kg, it was easy to find that PAHs concentrations in coal-like, coal cinder were significantly higher than in corresponding whole sediment. This

was in good agreement with observation of Ghosh et al. (2000) that the coal/wood-derived particles constituted only 5% of the sediment by weight but contained 62% of the total PAHs. It was also in accord with results by Rockne et al (2002) that 50-80% PAHs were associated with the low density fraction which represented only 3-15% of total sediment mass in the two sediments they studied.

Table 4.3 Concentrations (mg/Kg) of PAHs in coarse particles from Utica harbor sediment

Compound	Whole Sediment	Coal-like	Coal Cinder	Wood
Phe	6.5(±0.22)	177(±2.46)	291(±9.78)	49.1(±1.64)
Ant	5.8(±0.10)	74.3(±1.34)	334(±11.2)	25.4(±0.75)
Pyr	23.8(±0.45)	228(±5.01)	290(±8.65)	78.1(±1.39)
Chr	24.1(±1.03)	550(±20.3)	347(±10.3)	5.9(±0.23)
BbF	8.9(±0.31)	347(±12.9)	348(±15.2)	8.6(±0.31)
BkF	4.2(±0.05)	149(±5.21)	148(±4.89)	0.6(±0.05)
BaP	12.7(±0.36)	334(±13.7)	358(±7.81)	10.3(±0.42)
DBahA	7.6(±0.08)	268(±7.58)	425(±13.7)	8.4(±0.33)
BghiPe	5.4(±0.21)	79.3(±3.62)	198(±6.35)	6.7(±0.21)
Total	99.0	2207	2735	193.1

Table 4.4 Concentrations (mg/Kg) of PAHs in coarse particles from Rouge River sediment

Compound	Whole sediment	Coal-like	Coal Cinder	Wood
Phe	22.9(±0.48)	24.1(±0.50)	58.7(±1.06)	15.7(±0.35)
Ant	8.10(±0.23)	3.4(±0.05)	9.3(±0.31)	2.8(±0.11)
Pyr	36.5(±1.25)	37.8(±1.19)	94.9(±2.24)	2.0(±0.07)
Chr	22.4(±1.01)	3.4(±0.16)	168.5(±4.39)	4.6(±0.16)
BbF	15.4(±0.54)	3.2(±0.13)	53.3(±1.97)	2.0(±0.06)
BkF	8.80(±0.37)	1.1(±0.04)	60.4(±1.68)	2.2(±0.04)
BaP	11.6(±0.28)	2.7(±0.1)	68.9(±1.72)	3.5(±0.08)
DBahA	21.2(±0.46)	-	63.5(±1.59)	-
BghiPe	14.5(±0.32)	-	11.4(±0.52)	1.6(±0.04)
Total	161.4	75.7	589.0	34.4

4.3.2Sorption of phenanthrene to different particles in Utica Harbor sediment

Coarse particles from Utica Harbor sediment were used to conduct the sorption experiment to investigate the rate and extent of sorption of HOCs into different particles. Particles from Utica Harbor sediment were selected due to the ease of obtaining coarse particles in that the sediment had not been sieved before it was received as stated afore.

Table 4.5 Sorption of phenanthrene onto different coarse particles from Utica Harbor sediment

Particles	Initial Concentration on particle	Adsorbed after 1 day	Adsorbed after 2 days
Coal-like	177(±9.5)	24.7	27.3
Coal-like, Crushed	177(±9.5)	44.7	44.8
Coal Cinder	287(±13.7)	20.7	21.5
Coal Cinder, Crushed	287(±13.7)	22.2	22.3
Wood	49.1(±2.3)	162	163
Charcoal	25.7(±0.9)	133	143

The sorption of phenanthrene onto these particles showed different rate and extent for different particles as indicated in Table 4.5, which was resulted from the variation of properties for these particles. Table 4.5 showed that the adsorption of phenanthrene onto coal-like and coal cinder particles were much slower than that onto woody and wood charcoal particles. Two reasons were responsible for this observation—first, equilibrium limitation and second, kinetic limitation. Notice that the total concentrations after two days adsorption for

66

each category of particles were still far less than the adsorption capacities despite high initial concentration of contaminants coal-like and coal cinder particles, this suggests that the adsorption of phenanthrene to those particles were not limited by the equilibrium adsorption capacity. On the other hand, the diffusion rate of phenanthrene into coal-like particle matrix is very slow in that coal-like particle is much less porous with a total pore volume of $0.01cm^3/g$ (Jonker and Koelmans 2002), thus the second reason plays a much more important role leading to the above observed results.

4.3.3 Apparent partition coefficients of contaminants in different particles and pH value effects

Apparent partition coefficients of a series PAHs in coal-like and coal cinder particles were measured under different pH value conditions to investigate physical availability of HOCs associated with black carbon particles in sediments. In order to make the data comparable to the apparent partition coefficients measured for the whole Utica Harbor sediment, coal-like and coal cinder particles in this experiment were ground and passed through 2mm sieve after the coarse particles were obtained from original Utica Harbor sediment.

Apparent partition coefficients of PAHs in coal-like particles and coal cinder particles under pH value of 7.5 and 10 are presented in Table 4.6. It is shown that apparent partition coefficients of PAHs in both coal-like and coal cinder particles at neutral condition (pH of 7.5) were significantly greater than theoretical data estimated from LogKow using correlation reported in Karickhoff *et al.* (1979). This was not surprising in that it confirmed the argument of (Luthy, and other groups) that black carbon acted as sorbent and sequestered HOCs from

sediment. It was also consistent with observation of Jonker and Koelmans (2002) that various

soot and soot-like materials had much greater partition coefficient.

Table 4.6 Apparent partition coefficients of PAHs in coal-like and coal cinder particles from Utica Harbor sediment and pH value effect

Compound	Log Koc[a]	Coal-like[b]			Coal Cinder[c]		
		Conc mg/kg	Log Koc @ pH 7.5	Log Koc @ pH 10	Conc mg/kg	Log Koc @ pH 7.5	Log Koc @ pH 10
Phe	4.36	177	5.23	4.11	291	5.10	5.01
Ant	4.33	74.3	5.40	4.56	334	5.07	5.22
Pyr	4.97	228	5.01	4.66	290	5.25	5.28
Chr	5.65	550	6.35	5.60	347	6.62	6.72
BbF	5.59	347	6.23	5.30	348	6.79	6.74
BkF	5.79	149	6.14	5.52	148	6.56	6.58
BaP	5.83	334	6.32	5.71	358	6.86	6.58

c. Log Koc calculated from LogKow compiled in Mackay et al. 1991 using correlation reported Karickhoff *et al*. 1979 (LogKoc = 1.0 * LogKow – 0.21);
d. f_{oc} for coal-like particles from Utica sediment is 80.9%, focSoft is 39.4% and focHard is 41.5%;
e. f_{oc} for coal cinder particles from Utica sediment is 28.8%, focSoft 7.4%is focHard is 21.4%.

For the case of pH value of 10, the apparent partition coefficients of PAHs in coal-like particles measured were roughly equal to the LogKoc values estimated from LogKow using correlation reported in Karickhoff *et al.* (1979) and significantly less than those measured at pH value of 7.5, the difference ranged from a half to one logarithmic unit. It was, however, different for coal cinder particles because the apparent partition coefficients measured at pH value of 7.5 and 10 were roughly equal showing no significant pH value effect as observed for coal-like particles.

Humic acid could be dissolved under basic condition as reported in Mayer et al. 1993. Note that amorphous carbon content for coal-like particles was greater than coal cinder particles, it was possible that some amorphous organic carbon in coal-like particles such as humic acid dissolved in aqueous phase under basic condition, which decreased the association of PAHs with coal-like particles and increased PAHs in aqueous phase. Thus, the apparent partition coefficients of PAHs in coal-like particles under basic condition were significantly less than those under neutral condition.

4.3.4 Apparent partition coefficients of contaminants in field-contaminated sediments and in condensed phase organic carbon

The correlation of apparent partition coefficients of contaminants in coal-like and coal cinder particles from Utica Harbor sediment determined under neutral condition are shown in Figure 4.1. The apparent partition coefficients for all compounds in coal-like particles and coal cinder particles were roughly equal as shown in the figure because the points distributed along the 45 degree diagonal line. This was not difficult to understand because condensed phase organic carbon dominated both categories of particles under neutral condition which was close to the reality in the natural environment. In this context, the average of apparent

partition coefficients in coal-like and coal cinder particles was a good indication of apparent

partition coefficients for contaminants in condensed phase organic matter.
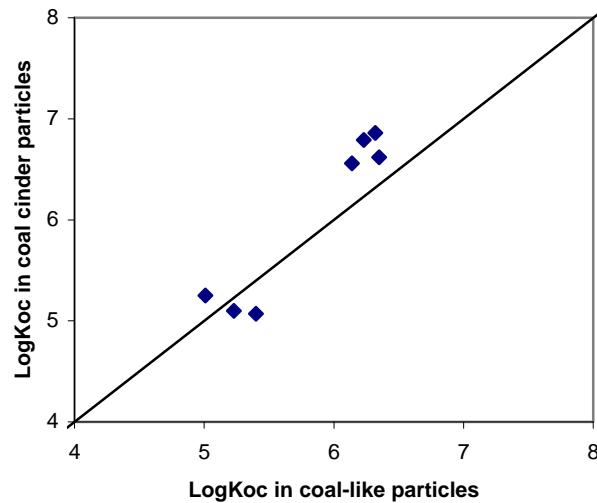
Figure 4.1 Correlation of apparent partition coefficients of contaminants in coal-like and coal cinder particles from Utica Harbor sediment.

Comparison of apparent partition coefficients of contaminants in bulk sediment and resistant fraction in Utica Harbor sediment with those in condensed phase organic carbon particles in neutral condition as indicated by the average of apparent partition coefficients of contaminants in coal-like and coal cinder particles is shown in Figure 4.2. The apparent partition coefficients of contaminants in bulk Utica sediment were in good accordance with the apparent partition coefficient in condensed phase organic carbon particles in neutral condition. This seemed to be contradictive to the previous argument that the labile fraction controls the short-term release contaminants and that the apparent partition coefficient would

be much less than the apparent partition coefficient in condensed phase organic carbon. However, the average fast desorption fraction of 0.28 for Utica sediment suggested that the dominant fraction was the sequestered fraction or desorption-resistant fraction which gave the apparent partition coefficient for bulk sediment almost the same as the apparent partition coefficient in condensed phase organic carbon. Since the apparent partition coefficients were not determined in true equilibria, thus, the apparent partition coefficients of contaminants in bulk Utica Harbor sediment were not linear combination of the apparent partition coefficients for the amorphous and condensed phase organic carbon according to the amorphous and condensed phase organic carbon contents.

On the other hand, the apparent partition coefficients of contaminants for the desorption resistant fraction were higher than the apparent partition coefficient in condensed phase organic carbon. This was not surprising because a small fraction of the contaminants associated with condensed phase organic carbon but easily desorbed was removed during the XAD2 treatment which directly resulted in the elevation of the apparent partition coefficients. Similar results were also obtained for Rouge River sediment as shown in Figure 4.3.
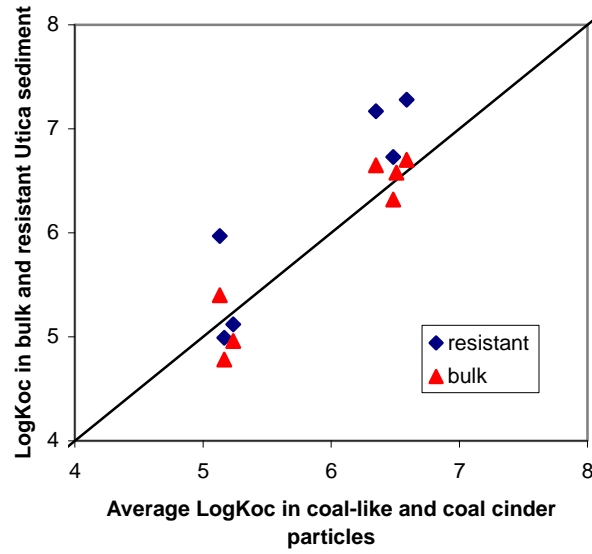
Figure 4.2 Comparison of apparent partition coefficients of contaminants in Utica Harbor sediment and in condensed phase organic carbon particles
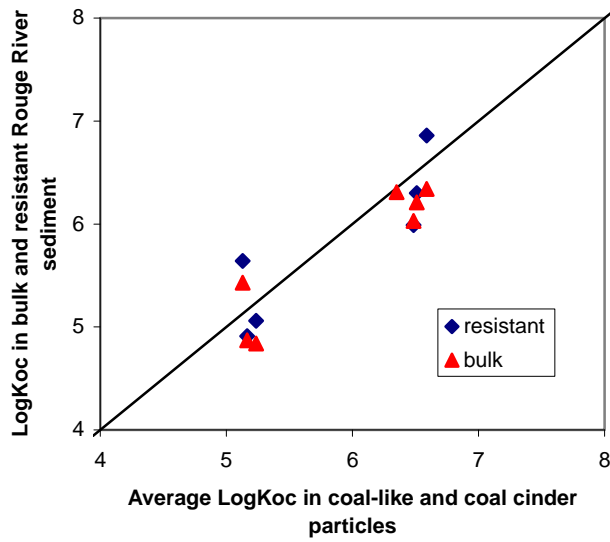
Figure 4.3 Comparison of apparent partition coefficients of contaminants in Rouge River sediment and in condensed phase organic carbon particles

4.4 Summary

Chemical analysis of coarse particles from different sediments showed great variation in concentrations of PAHs, with total PAHs concentration up to 2,735 mg/Kg. Generally, PAHs concentrations in coarse particles were significantly higher than those in corresponding whole sediments. This was in good agreement with observations reported in Ghosh et al. (2000) and Jonker et al (2002) that PAHs contamination in sediments was predominantly associated with black particles.

Phenanthrene adsorption experiment onto coarse particles showed various sorption rates. Slow sorption rate was observed for coal-like particles. Difficulty for diffusion of phenanthrene into coal-like particles was most likely the reason leading to the slow adsorption rate.

Apparent partition coefficients of PAHs associated with coal cinder particles under basic condition were roughly equal to those under neutral condition, which was contrary to coal-like particles. Apparent partition coefficients of PAHs associated with coal-like particles under basic condition were significantly less than those under neutral condition. It was most likely due to dissolution of amorphous organic carbon from coal-like particles such as humic acid into aqueous phase under basic condition.

The apparent partition coefficients of PAHs in condensed phase organic carbon particles were a good indication of the apparent partition coefficients in the bulk Utica Harbor and Rouge River sediment. The apparent partition coefficients of contaminants in bulk Utica Harbor sediment were not linear combination of the apparent partition coefficients for the amorphous and condensed phase organic carbon according to the amorphous and condensed

73

phase organic carbon contents because the apparent partition coefficients were not determined

in true equilibria.

CHAPTER 5 MODELING ACTIVITIES

5.1 Introduction

It has been well acknowledged that the sorption and desorption of contaminants from natural sorbents were biphasic. The desorption resistance has been ascribed to the heterogeneity of organic matter in sediments.

The biphasic desorption kinetics could be modeled using a two compartment first-order kinetic model (Karickhoff, 1980; Hawthorne, 2001), but this kinetic model did not provide information on the mechanisms behind the biphasic desorption behavior. Some mechanistic models, e.g., Distributed Reactivity Model (Weber et al. 1992), Dual Mode Model (Xing, et al., 1996), biphasic models (Kan et al., 1998; Gustafsson et al., 1997), were proposed to address equilibrium sorption and desorption behavior of HOCs in sediments. However, the reality is that the diffusion or migration of contaminants in condensed phase organic matter is an extremely slow process and it cannot reach equilibrium even after years (Ghosh et al., 2001). Thus, a model that includes both equilibrium effects and kinetic effects is needed to estimate the physical partition of contaminants in sediment water systems. Two domain diffusion model were utilized by Rockne et al. (2002) to fit there desorption data. However, the assumption that PAHs were initially uniformly distributed throughout sediment aggregates undermined their efforts because microscopic observations showed that PAHs only resided in a very thin layer near external surface of the coal-derived particles in the sediment (Ghosh et al., 2001).

This chapter focused on the development of a predictive model of sorption/desorption behavior of HOCs in the natural sorbents in the environment, which enabled us to estimate the

effective partition of HOCs between sediment and pore water and included both equilibrium effects and kinetic effects.

5.2 Development of the model

5.2.1 Structure of the model

The sequestration behavior of organic contaminants in sediments has been attributed to the heterogeneity of soil/sediment organic matter. Amorphous organic carbon exhibits less sorption capacity and fast kinetics while condensed phase organic carbon exhibits greater sorption capacity and slow kinetics. The partitioning and sequestration behaviors of contaminant in sediment represent the balance between the kinetics and capacity of various organic carbon matrices in sediment. The slow kinetics is most likely attributed to the slow diffusion of contaminants in the condensed phase carbon. Fig.6.1 characterizes schematically amorphous and condensed phase SOM in sediment.
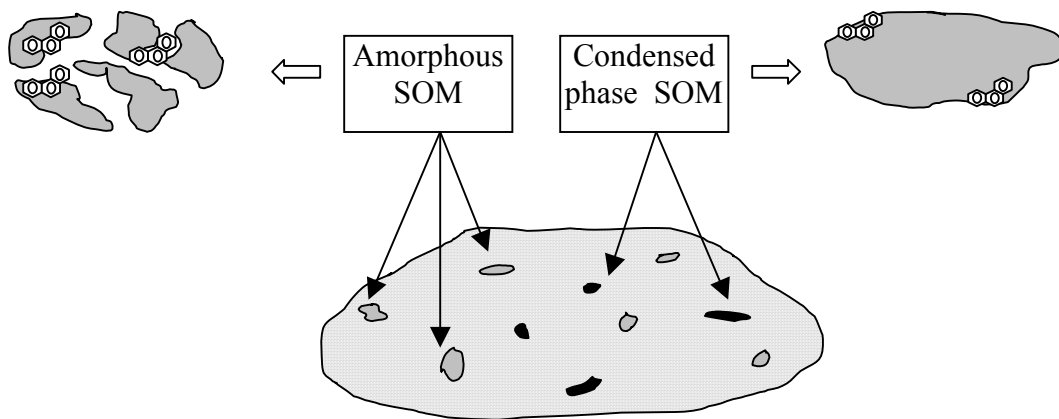
Figure 5.1 Amorphous and condensed phase organic matter in sediment

The model is based on the following major assumptions:

1. Contaminants are mostly associated with sediment/soil organic matter.

2. Soil/sediment organic matter is classified as two broad categories--amorphous and condensed phase organic carbon. Amorphous organic carbon is physically loose having a lower adsorption capacity and faster effective diffusivity for contaminant, condensed carbon is physically compact having a greater adsorption capacity and a slower effective diffusivity for contaminants;

3. Contaminant in intraparticle pore water is locally in equilibrium with contaminant sorbed in solid phase, with organic carbon normalized partition coefficient K_{oc}.

4. Sorption capacity of organic matter for contaminant is characterized by the organic carbon normalized partition coefficient Koc;

5. Contaminants migrate in sediment organic matter particles by retarded diffusion.

Governing equation for amorphous organic matter is

$$\frac{\partial C_A}{\partial t} = \frac{D_{eff}^A}{R_f^A} \frac{\partial^2 C_A}{\partial x^2}$$ (5.1)

where

C_A is contaminant concentration in soft organic matter pore water (mg/L),

D is the diffusivity of contaminant in water (m^2/s),

ε is the porosity of soft organic matter,

ρ_A is the bulk density of soft organic matter (kg/L),

OC_A is the organic carbon content of soft organic matter,

$K_{OC}{}^A$ is the organic carbon normalized partition coefficient of contaminant in soft organic matter,

R_f^A is retardation factor for soft organic matter,

$D_{eff}{}^A$ is the effective diffusivity of contaminants in soft organic matter.

And

$$D_{eff}^A = D \cdot \varepsilon^{4/3} \tag{5.2}$$

$$R_f^A = \varepsilon + \rho_A \cdot K_{OC}^A \cdot OC_A \tag{5.3}$$

Governing equation for condensed phase organic matter is

$$\frac{\partial C_S}{\partial t} = D_A^C \frac{\partial^2 C_S}{\partial x^2} \tag{5.4}$$

Where C_S is contaminant concentration in condensed phase organic matter (mg/kg), D_A^C is the diffusivity of contaminant in condensed phase organic matter (m^2/s).

If we define

$$C_S' = \frac{C_S}{K_d^C} = \frac{C_S}{K_{OC}^C \cdot OC_C} \tag{5.5}$$

equation (6.4) can be rewritten as

$$\frac{\partial C_S'}{\partial t} = D_A^C \frac{\partial^2 C_S'}{\partial x^2} \tag{5.6}$$

where

OC_C is the organic carbon content of condensed phase organic matter,

$K_{OC}{}^C$ is the organic carbon normalized partition coefficient of contaminant to condensed phase organic matter.

Equation (6.1) and equation (6.6) will be used to solve for $C_A(x, t)$ and $Cs'(x, t)$ given different boundary conditions and initial conditions for sorption, desorption, portioning and aging processes. Contaminant concentration in sediment will be quantified from $C_A(x, t)$ and $Cs'(x, t)$.

5.2.2 Parameters for the model

Parameters included in the model and their descriptions are listed in Table 6.1.

Table 5.1 Denotation of parameters used in the model

Symbol	Description
ε	Porosity of amorphous organic matter
D	Diffusivity of contaminant in pure water
$D_A{}^C$	Diffusivity of contaminant in condensed phase organic matter
K_{oc}	Contaminant organic carbon normalized partition coefficient of amorphous and condensed phase organic matter
ρ	Density of amorphous and condensed phase organic matter
OC	Organic carbon content for amorphous and condensed phase organic matter
f_{oc}	Total organic carbon content in sediment
$f_{oc}{}^C$	Condensed phase organic carbon content in sediment

$f_{oc}{}^A$	Amorphous organic carbon content in sediment
(V/A)	Volume to surface area ratio, represents a half of characteristic length of amorphous and condensed phase organic matter particle

In the model, the diffusivity of contaminant in condensed phase organic matter, the volume/surface area ratio for condensed phase organic matter will be obtained by fitting the experimental data. All other parameters will be obtained either from literature or from experimental measurement as shown in Table 6.2.

Table 5.2 Source of parameters used in the model

Symbol	Description
ε	$\varepsilon \sim 0.4$ (Assumed)
D	$7.74*10^{-10}$ m^2/s for phenanthrene (USEPA, 1996)
$D_A{}^C$	Fitting
K_{oc}	$10^{4.4}$ for phenanthrene in amorphous carbon (Measured) $10^{5.0 \sim 6.0}$ for phenanthrene in condensed phase carbon (Jonker, 2002)
ρ	1.5 for amorphous and 2.0 for condensed phase organic matter (assumed)
OC	0.58 for amorphous and 0.9 for condensed phase organic matter (measured)
f_{oc}	Measured

$f_{oc}{}^C$	Measured
$f_{oc}{}^A$	Measured
(V/A)	Assumed 20μm for amorphous organic matter, For condensed phase organic matter $(V/A) = 1/(\rho_C * a)$, where a is surface area per unit mass and will be determined by fitting.

These partial differential equations with corresponding boundary conditions and initial conditions were solved simultaneously utilizing finite element method (Refer to Appendix I for detailed computational methods) and Matlab program was written to implement the computation needed for the model (Refer to Appendix II for MatLab codes).

For simple, the shape of the organic matters is assumed to be infinite slab with thickness of the characteristic length which is indicated by the volume to surface ratio of the amorphous and condensed phase organic matter. This assumption is appropriate because the sorption and desorption results do not depend on specific shape of the particle once the characteristic length of the particle is expressed by volume to surface area ratio. Figure 6.2 and 6.3 represent the sorption progress of a slab and sphere particle at 1hour and 100 hour respectively and it is obvious that particle shape does not control the sorption progress.
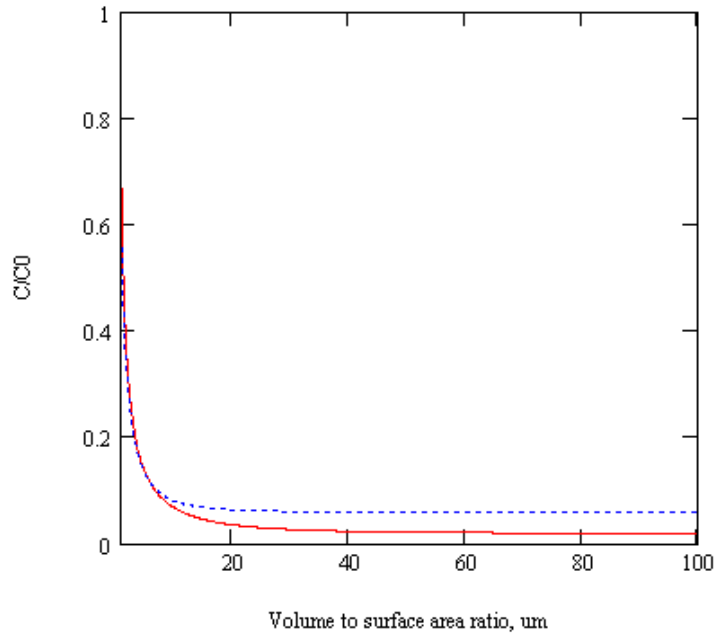
Figure 5.2 Comparison of sorption progress of slab and sphere at 1 hour
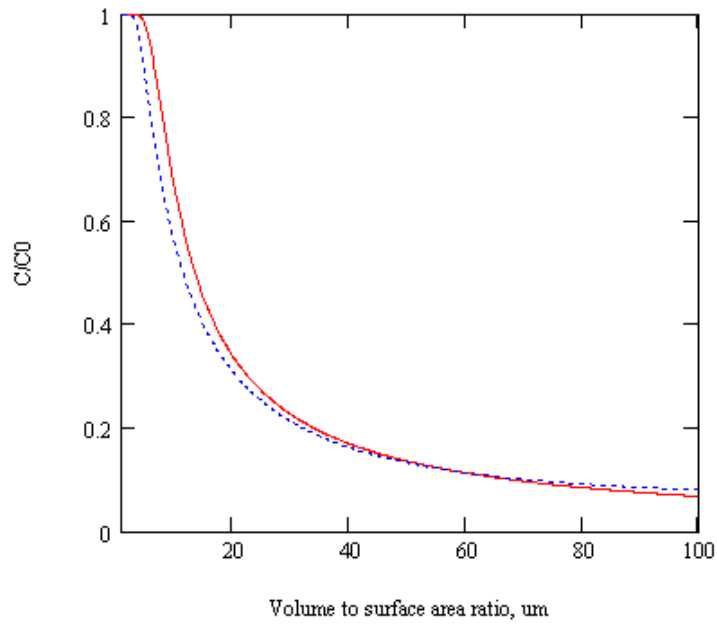
Figure 5.3 Comparison of sorption progress of slab and sphere at 100 hours

5.2.3 Modeling individual process

5.2.3.1 Adsorption process

In adsorption process, sediment organic matter was assumed to pick up contaminants continually from the sediment porewater and the porewater concentration keeps constant which was appropriate for our inoculation process and for most of field contamination process. Boundary conditions and initial condition for adsorption process are as follows.

Boundary conditions for amorphous organic matter,

$$\begin{cases} \dfrac{\partial C_A}{\partial x} = 0 & \text{at x=0} \\ C_A = C_{init} & \text{at x=} \pm \text{(V/A)} \end{cases} \quad (5.7)$$

and for condensed phase organic matter,

$$\begin{cases} \dfrac{\partial C_S{}'}{\partial x} = 0 & \text{at x=0} \\ C_S{}'= C_{init} & \text{at x=} \pm \text{(V/A)} \end{cases} \quad (5.8)$$

where C_{init} is the initial concentration of contaminant in water. Initial conditions were $C_S{}'= 0$ and $C_A = 0$.

The modeling of phenanthrene in a model sediment with organic carbon content of 2%, among which 0.2% is amorphous organic carbon and 1.8% is condensed phase organic carbon, was utilized to demonstrate the model. The modeling results for different individual processes in this section including sorption, desorption, aging and apparent desorption isotherms were all obtained based on this model sediment.

83

If the initial phenanthrene concentration in sediment porewater before adsorption is 1 mg/kg and it keeps constant during the adsorption period. The intraparticle pore water concentration profile of phenanthrene in amorphous organic matter particle and Cs' profile in condensed phase organic matter particle at different time instance during adsorption are shown in Figure 6.4, it is obvious that phenanthrene was saturated in intraparticle aqueous phase in amorphous organic matter after a short time of adsorption while it is far from equilibrium for condensed phase organic matter even at the end of adsorption.
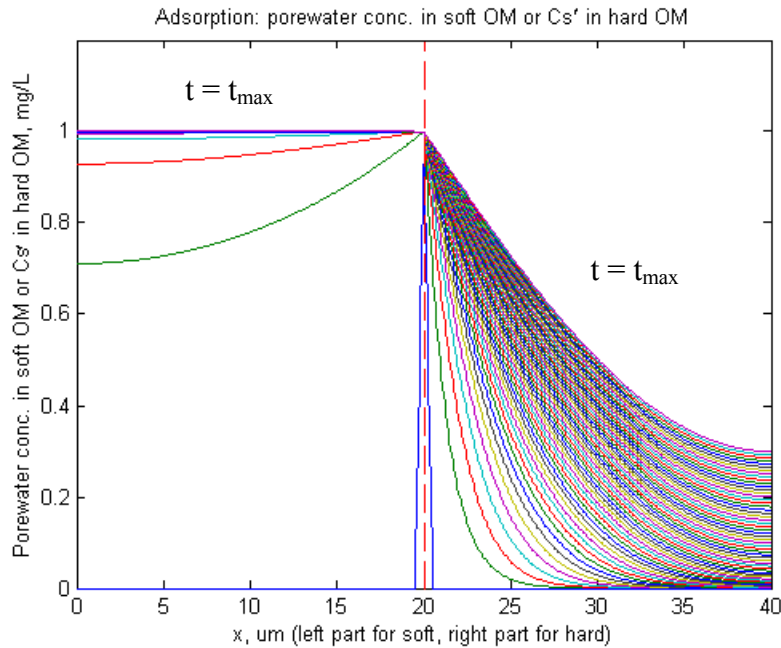
Figure 5.4 Modeling phenanthrene concentration profile in intraparticle porewater in amorphous organic matter particle and Cs' in condensed phase organic matter particle at different time instance during adsorption in model sediment. Left half denotes amorphous organic matter particle, right half denotes condensed phase organic matter particle.

The phenanthrene concentration in sediment with respect to adsorption time during adsorption process is presented in Figure 6.5. The phenanthrene concentration in sediment raised dramatically in the early stage of the adsorption period because the amorphous organic

matter reached its saturation adsorption capacity and then it increased very slowly while the condensed phase organic matter was still picking up phenanthrene from the sediment porewater.
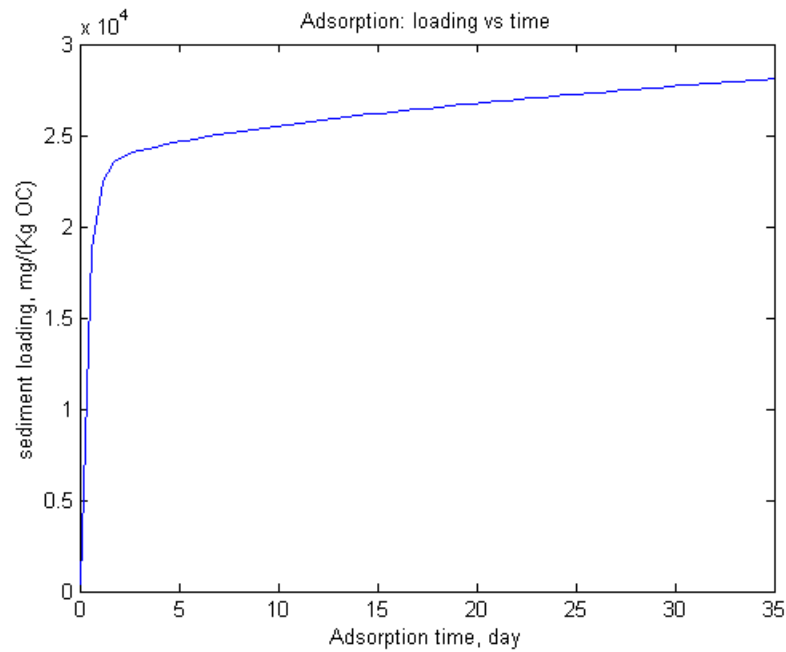
Figure 5.5 Modeling phenanthrene concentration in solid phase for adsorption process in model sediment

5.2.3.2 Desorption process

In the desorption period, the phenanthrene concentration in sediment porewater was assumed to be essentially zero and it was appropriate in that in most cases, strong sorbents were used as infinite sink to keep the porewater concentration to be zero to maintain maximum driving force for desorption. Boundary conditions for desorption process are stated below.

For amorphous organic matter,

$$
\begin{cases}
\dfrac{\partial C_A}{\partial x} = 0 & \text{at x=0} \\
C_A = 0 & \text{at x=} \pm (V/A)
\end{cases}
\tag{5.9}
$$

and for condensed phase organic matter,

$$
\begin{cases}
\dfrac{\partial C_S{}'}{\partial x} = 0 & \text{at x=0} \\
C_S{}' = 0 & \text{at x=} \pm (V/A)
\end{cases}
\tag{5.10}
$$

Initial concentration C_A and C_S' were the results at the end of adsorption process. Modeling of porewater concentrations in amorphous OM or Cs' in condensed phase OM at different time instance during desorption process for model sediment are shown in Figure 6.6. On the x axis, the position at 0 μm represents the center of amorphous organic matter, position at 20 μm represents the surface of both amorphous and condensed phase organic matter, and position at 40 represents the center of condensed phase organic matter. From the phenanthrene concentration profile in condensed phase organic matter, the migration of phenanthrene in both directions to the surface and the center of the particle is observed. This might explain why the desorption process usually takes longer time than adsorption to reach steady state.

Figure 5.6 Modeling of porewater concentration in amorphous OM or Cs' in condensed phase OM at different time instance during desorption for model sediment.

Modeling results for desorption of phenanthrene from model sediment are shown in Figure 6.7. It is consistent with biphasic desorption curve depicted in Hawthorne et al (2001).

Figure 5.7 Modeling desorption kinetics of phenanthrene from model sediment.

5.2.3.3Apparent partition coefficient and desorption isotherms

Desorption isotherm was established in the following way. A series of sediments with different contaminant concentrations along the desorption kinetics curve as the desorption process advanced further. The apparent partition coefficient of contaminants in each sediment along the desorption kinetics was estimated. These sediment concentrations and corresponding aqueous phase concentrations at the end of apparent equilibration were used to generate the desorption isotherm.

Apparent partition coefficient is estimated based on batch equilibration for the model sediment, with water to solid mass ratio of 60g to 1g. Equilibration time of 10 days and 60 days are used to estimate the apparent partition coefficient for freshly inoculated sediment to evaluate the effect of equilibration time on apparent partition coefficient.

Boundary conditions for apparent partition coefficient estimation are

$$
\begin{cases}
\dfrac{\partial C_A}{\partial x} = 0 & \text{at x=0 for soft organic matter} \\[2ex]
\dfrac{\partial C_S{'}}{\partial x} = 0 & \text{at x=0 for hard organic matter} \\[2ex]
\dfrac{\partial C_w}{\partial t} = -\dfrac{D_{eff}{}^{soft}}{v_1}\dfrac{\partial C_A}{\partial x}\bigg|_{x=(V/A)_{soft}} + \dfrac{D_A{}^{hard}Koc^{hard}OC_{hard}\rho_{hard}}{v_2}\dfrac{\partial C_S{'}}{\partial x}\bigg|_{x=-(V/A)_{hard}} \\
\qquad\text{at the interface of organic matter and water}
\end{cases}
\tag{5.11}
$$

Where v_i (i=1,2) is the ratio of water to organic matter by volume for amorphous and condensed phase organic matter respectively, C_w is aqueous concentration of contaminant. And

$$v_1 = Ratio^{w-s} \cdot \frac{\rho_{soft}}{\rho_{water}} \cdot \frac{OC_{soft}}{f_{oc}{}^{soft}} \cdot \left(\frac{V}{A}\right)_{soft} \tag{5.12}$$

$$v_2 = Ratio^{w-s} \cdot \frac{\rho_{hard}}{\rho_{water}} \cdot \frac{OC_{hard}}{f_{oc}{}^{hard}} \cdot \left(\frac{V}{A}\right)_{hard} \tag{5.13}$$

where $Ratio^{w-s}$ is the mass ratio of water to sediment.
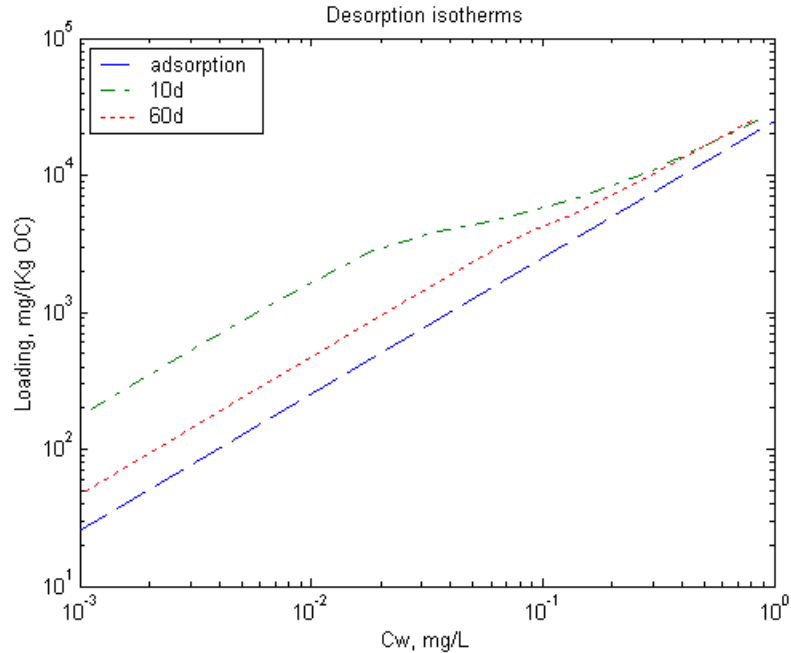
Figure 5.8 Modeling result of desorption isotherms of phenanthrene in freshly inoculated model sediment at equilibration time of 10 days and 60 days.

The desorption isotherms determined at equilibration time of 10 days and 60 days were shown in Figure 6.8. The results show that incubation time plays an important role to determine the desorption isotherms. Desorption resistance may not be observed if the equilibration time is long enough for contaminants to reach real equilibrium in the re-distribution process in the water sediment batch system. These desorption isotherms were similar in shape as the biphasic desorption isotherms reported in Kan et al. (1998), the difference is that the model presented in this dissertation was able to predict the effect of

equilibration time on the apparent partition coefficient and was able to predict the aging effect which will be discussed below.

5.2.3.4 Modeling the aging effects

Aging process was modeled as wet sediment was stored for a certain period, 1000 days in this case, after the adsorption process. Boundary conditions are the same as those for estimation of apparent partition coefficient. The only difference is that the aging process has a very small water to solid ratio, with sediment moisture content of about 40% of wet sediment, which means that water to solid ratio is about 0.67g to 1g. The initial condition for aging process is the endpoint of adsorption process. Model demonstration of porewater concentration in amorphous OM or Cs' in condensed phase OM at different time instance during aging process for model sediment is shown in Figure 6.9. The contaminants migrated from amorphous organic matter into condensed phase organic matter at a very slow speed during the aging process.
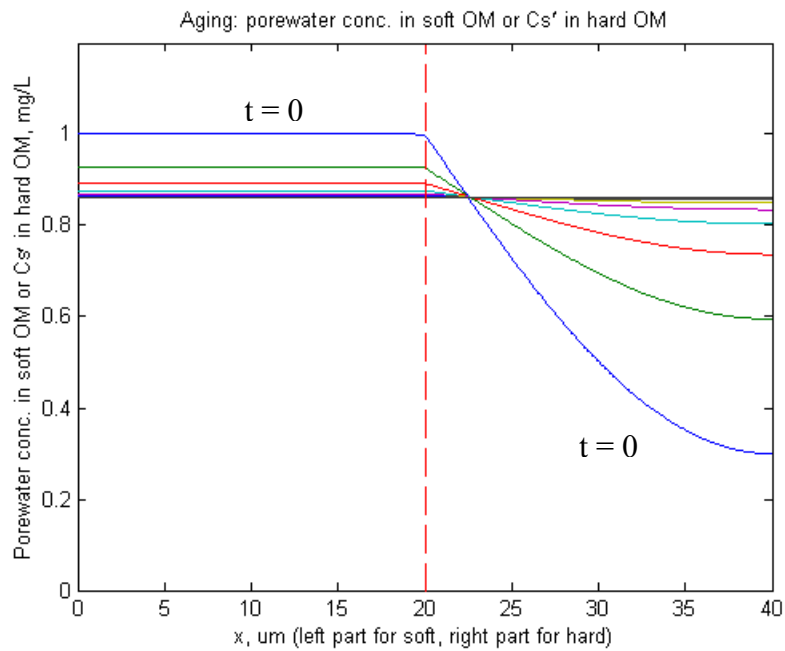
Figure 5.9 Model demonstration of porewater concentration in amorphous OM or Cs' in condensed phase OM at different time instance during aging process in model sediment.

Desorption kinetics were obtained after the aging process, assuming zero concentration in sediment porewater. Figure 6.10 shows modeling results for desorption kinetics with the aging effect. A larger fraction of contaminants remaining in aged sediment than in freshly-inoculated sediment.
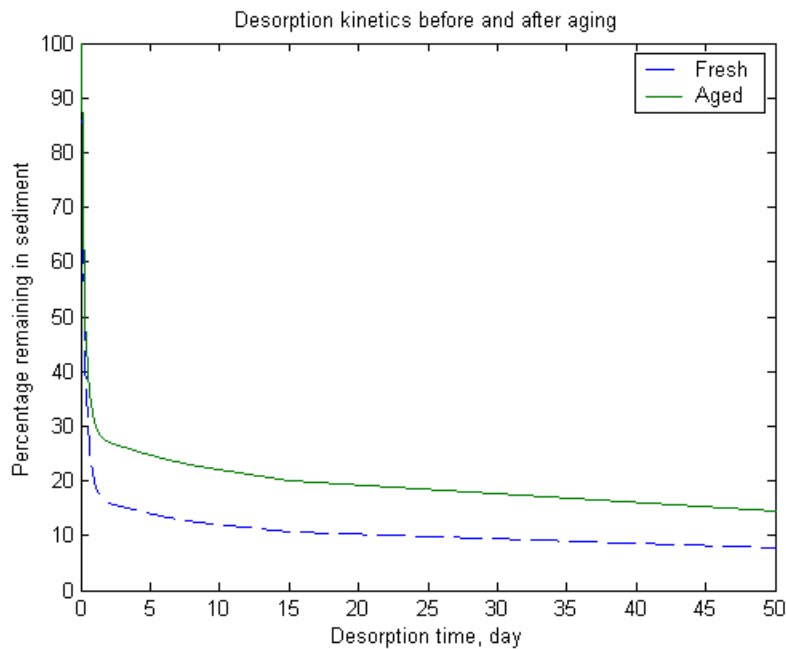
Figure 5.10 Modeling desorption kinetics of phenanthrene from freshly inoculated and aged (for 1000 days) model sediment.

Figure 6.11 shows modeling results for the desorption isotherms for freshly inoculated and aged model sediment. In this figure, the aging effect on the desorption resistant phenanthrene concentration was represented by higher desorption resistant phenanthrene ($q_{res,aged} > q_{res,fresh}$) because contaminants slowly migrated into the condensed phase organic matter particles from amorphous organic matter particles through the sediment porewater as a connection between those two categories of particles.
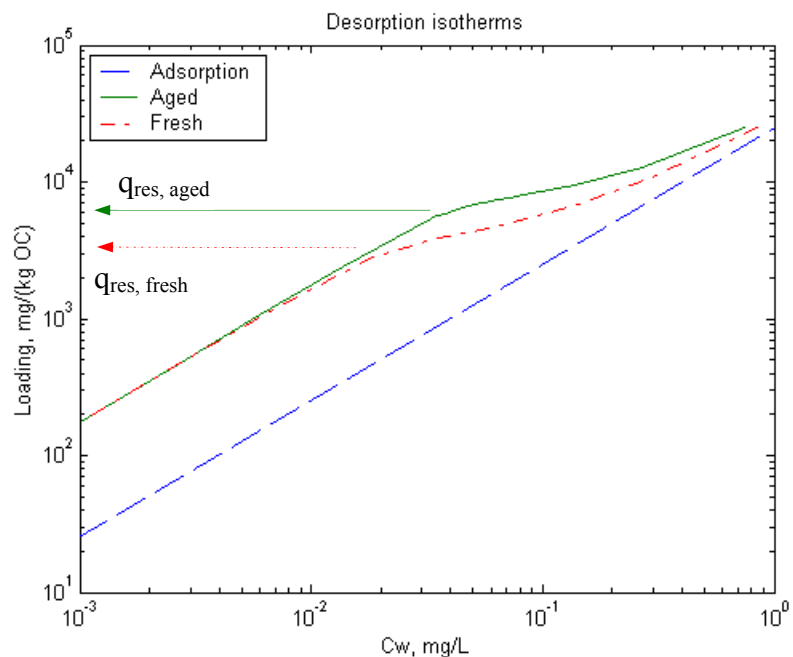
Figure 5.11 Modeling desorption isotherm of phenanthrene in freshly inoculated and aged (for 1000 days) model sediment.

5.3 Modeling Results and Discussion

5.3.1Lab-inoculated sediment

Modeling results for desorption kinetics of phenanthrene in freshly inoculated and aged Bayou Manchac sediment determined in chapter 2 were shown in Figure 6.12.
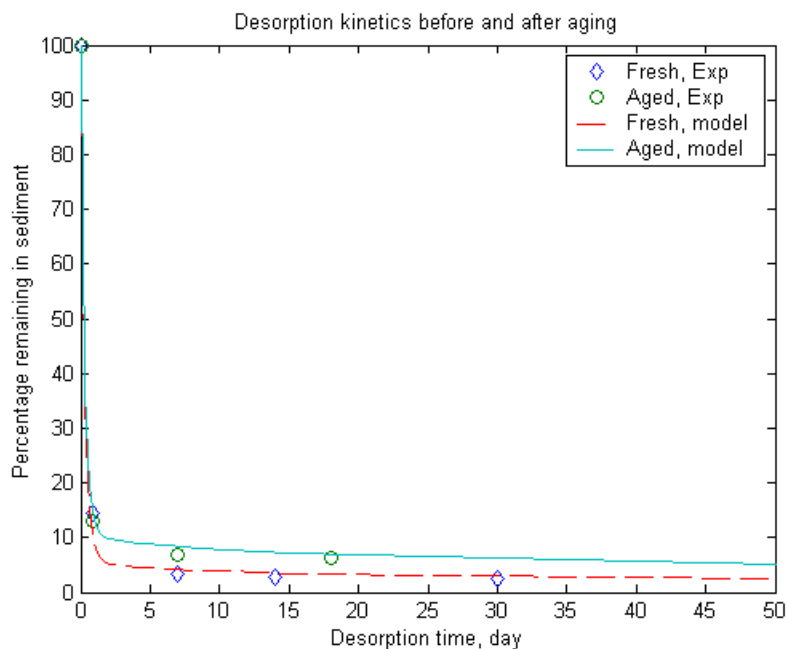
Figure 5.12 Modeling results for desorption kinetics of phenanthrene in freshly inoculated and aged Bayou Manchac sediment.

The model predicted desorption kinetics were obtained from the following parameters. The adsorption time was 35 days which was the inoculation time for the experiment. Desorption time was selected to be 600 days to make sure that the concentration remaining in sediment was low enough and it covered the scope of the desorption experiment. The diffusivity of phenanthrene in water was $7.7*10^{-10}$ m^2/s (Assumed same as anthracene because of identical molecular weight, diffusivity for anthracene from USEPA, 1996). The logarithm of organic carbon normalized partition coefficient of phenanthrene in amorphous and condensed phase organic matter were 4.4 (Calculated from LogKow compiled in Mackay et al. 1991 using correlation reported Karickhoff *et al*. 1979 (LogKoc=1.0*LogKow–0.21)) and 5.0 (Jonker and Koelmans, 2002 reported much higher value which is greater than 6, 5.0 was taken to match our measurement for desorption resistant partition coefficient) respectively. Organic carbon contents of amorphous and condensed phase organic matter were 0.58 and 0.9

94

respectively. The densities of amorphous and condensed phase organic matter were 1.5 and 1.8 respectively. Porosity of amorphous organic matter was assumed to be 0.4. Total organic carbon content of Bayou Manchac sediment was 1.54%. If we assume the phenanthrene concentration in sediment porewater during the inoculation period to be the solubility of phenanthrene in water, which is 1.0 mg/L, the best fit for diffusivity of phenanthrene in condensed phase organic matter and volume to surface area ratio of condensed phase organic matter were $3.2*10^{-17}m^2$/s and $2.0*10^{-5}$ m with the amorphous and condensed phase organic carbon percentages out of total organic carbon content of 97% and 3% respectively.

Note that the measured amorphous and condensed phase organic carbon percentages out of total organic carbon content for Bayou Manchac sediment were 52% and 48%. There were many uncertainties leading to the discrepancy. One of the possible reasons was that the method to determine amorphous and condensed phase organic carbon content was not appropriate. Another possible reason was that phenanthrene might still be residing on the surface of the sediment particles in the form of crystals.

The modeling results for desorption isotherms for Bayou Manchac sediment determined in Chapter 2 were shown in Figure 6.13. Good agreement was achieved between the experimental data and model prediction. The basic parameters were the same as the desorption kinetics. The best fit results for diffusivity of phenanthrene in condensed phase organic matter was $2.2*10^{-17}m^2$/s and volume to surface area ratio was $2.0*10^{-5}m$ with the amorphous and condensed phase organic carbon percentages out of total organic carbon content of 99% and 1% respectively.
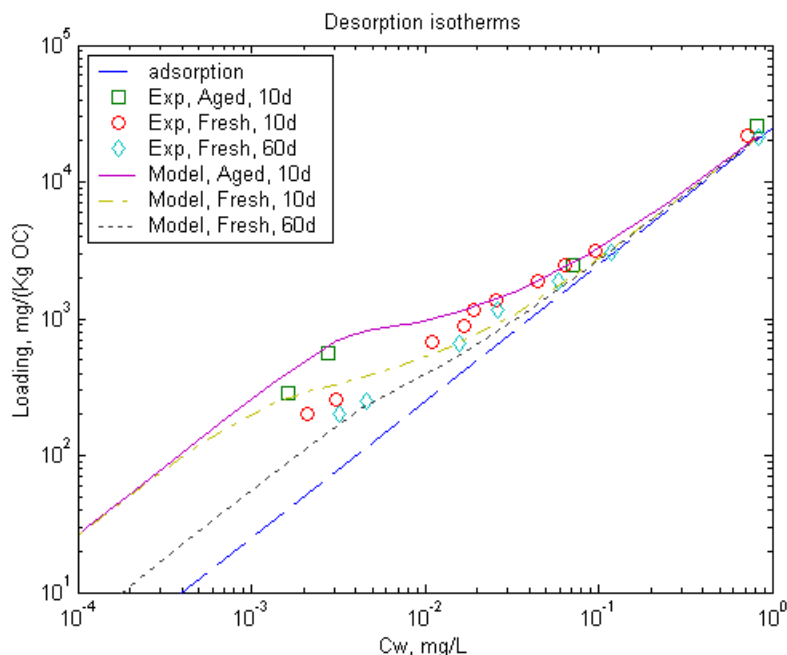
Figure 5.13 Modeling results of desorption isotherms for Bayou Manchac sediment determined at 10 days for freshly inoculated and aged sediment and at 60 days for freshly inoculated sediment

Initially, the experimental results were modeled with the desorption kinetics simultaneously using exactly the same set of parameters, which turned out to be not applicable because the obtaining of desorption isotherms for Bayou Manchac sediment involved in washing the sediment using the isopropanol/water solution to accelerate the desorption of phenanthrene from the sediment. The washing procedure was probably not consistent with the desorption procedure using XAD2 sorbent. The separate modeling effort for desorption kinetics and desorption isotherms gave acceptable results respectively.

5.3.2 Field contaminated sediments

The fast desorption fractions of selected PAHs determined for field contaminated sediment (Utica Harbor and Rouge River sediment) using XAD2 sorbent and the apparent partition coefficient of selected PAHs before and after XAD2 treatment were modeled

96

simultaneously. According to the contamination history, the contamination process was modeled as the sediment organic matter had been picking up contaminants from the aqueous phase for 50 years. The modeling and experimental results of fast desorption fraction operationally defined by the fraction removed using XAD2 sorbent in 20 hours for Utica Harbor and Rouge River sediment are shown in Figure 6.14. The experimentally determined fast desorption fractions for selected PAHs in both sediments were in good agreement with the model prediction as they distributed on the graph along the diagonal line which suggested that experimental value and model prediction were exactly identical.
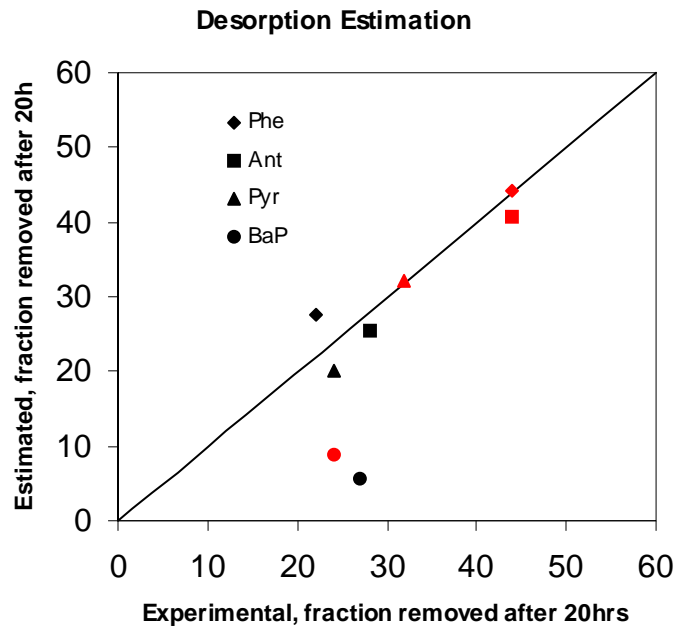
Figure 5.14 Experimental results and model prediction on the fast desorption fraction for selected PAHs in Utica Harbor and Rouge River sediment. Black points for Utica Harbor sediment, Red points for Rouge River sediment.

The measured and model predicted apparent partition coefficients for selected PAHs in Utica Harbor and Rouge River sediment before and after XAD treatment are shown in Figure 6.15. In general, the model predicted values were consistent with experimental data showing that the model was successful.
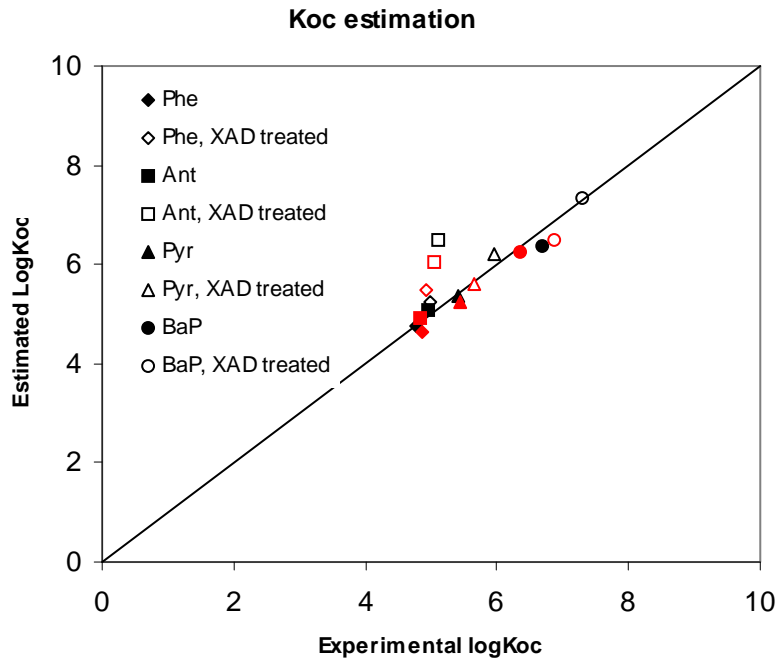
Figure 5.15 Experimental results and model prediction on the apparent partition coefficient for selected PAHs determined at 10days of equilibration time in Utica Harbor and Rouge River sediment. Black points for Utica Harbor sediment, Red points for Rouge River sediment.

The parameters for the modeling of Utica Harbor and Rouge River sediment are listed in Table 6.3. Our estimated diffusivities of selected PAHs in condensed phase organic matter ranged from $1.8\sim2.2*10^{-19}m^2/s$, the volume to surface area ratio were $1.5*10^{-5}m$. Surprisingly, the same set of parameters worked very well for both Utica Harbor and Rouge River sediment

even though they differed from each other by their total organic carbon content and amorphous/condensed phase organic carbon content.

Table 5.3 Parameters for Utica sediment

Compound	D (m^2/s)	Porosity	D_A^C (m^2/s)	VSRatio (m)	logKoc^A	logKoc^C	CwInit (mg/L)
Phe	7.70E-10	0.4	2.20E-19	1.50E-05	4.40	5.00	5.80E-03
Ant	7.50E-10	0.4	1.90E-19	1.50E-05	4.70	5.30	2.70E-03
Pyr	7.20E-10	0.4	2.00E-19	1.50E-05	5.00	5.6	5.50E-03
BaP	5.80E-10	0.4	1.80E-19	1.50E-05	6.00	6.6	3.00E-04

The extremely small diffusivities of PAHs in condensed phase organic matter estimated in this study were comparable to reported diffusivities of HOCs. Ghosh et al. (2001) estimated PAHs diffusivities in coal-derived particles at room temperature to be in the range from 10^{-17} to 10^{-19} cm^2/s. Carroll et al. (1994) calculated effective diffusivity for PCBs in the range of 10^{-20} to 10^{-21} cm^2/s in polymeric soil organic matter.

5.4 Summary

Both kinetics and equilibrium effect are included in the model to study the transport and sequestration of contaminants in sediments. The ability of the model to predict sorption/desorption behavior of HOCs in contaminated sediments suggest that slow diffusion process of HOCs in condensed phase carbon in sediment is most likely the reason leading to the biphasic desorption behavior and observed desorption resistance.

The model is able to predict biphasic desorption, desorption resistance and aging effect of PAHs in laboratory-contaminated sediments. The best fit results for diffusivity of

phenanthrene in condensed phase organic matter was $2.2*10^{-17}$ m^2/s and volume to surface area ratio was $2.0*10^{-5}$m.

The model is able to model fast desorption fraction and apparent partition coefficients of PAHs in field-contaminated sediments, with diffusivity in condensed phase carbon of $1.8\sim2.2*10^{-19}$ m^2/s for different compounds and volume/surface area of $1.5*10^{-5}$ m.

CHAPTER 6 CONCLUSIONS AND RECOMMENDATIONS

Conclusions:

- Desorption resistance for BM and UL sediments were not significantly different, though the two sediments have different soft and hard carbon contents. About 3 and 4% of the original saturated phenanthrene in BM and UL sediment were considered to be slow desorption fraction of desorption-resistant fraction according to the desorption kinetics determined using XAD2 nonpolar sorbent. These were comparable to the maximum irreversible concentration, q_{max}^{irr}, determined by fitting desorption isotherms using Kan et al's biphasic sorption/desorption model, which indicated that about 1.5% of the original saturated phenanthrene was desorption-resistant fraction. Aged sediment exhibited greater desorption resistance for both BM and UL sediment. Again no significant deviation on aging effects was observed for BM and UL sediments.

- The absence of correlation between desorption resistance and condensed phase organic carbon content in laboratory-inoculated BM and UL sediment was most likely due to the extremely slow diffusion rate of contaminant in condensed phase organic carbon. The time scale of 5 weeks for inoculation and two to three years of aging period were not long enough for a considerable amount of contaminant to migrate into the condensed phase organic carbon.

- Prolonged equilibration time for Bayou Manchac sediment exhibited less apparent partition coefficients. Different apparent partition coefficients with different equilibration time reflected that the slow diffusion of the contaminants into the hard carbon particles is most likely the cause to the result. The desorption resistance represented by the deviation of desorption curve from the projected adsorption line on desorption isotherms might not be real desorption resistance if long enough equilibration time were waited for the system to reach true equilibria.

- Fast desorption fraction of the same contaminant in different sediments varied a lot because of different sediment properties. Utica Harbor sediment, with higher condensed phase carbon content, exhibited lower fast desorption fraction than Rouge River sediment with lower condensed phase carbon content. The desorption resistant fractions as determined by XAD2 treatment for field-contaminated sediments were well connected to the condensed phase carbon content as defined by the combustion method at 375°C, greater condensed phase carbon content indicating less fast desorption fraction.

- Organic carbon normalized apparent partition coefficient for bulk sediment, resistant fraction and available fractions showed that only fast desorption fraction or called labile fraction of contaminants was available for short term equilibrium partitioning.

- Phenanthrene concentration in light fractions rich in organic matter were significantly greater than in light fraction rich in clay and silt and than in heavy fractions rich in sand.

- Availability of phenanthrene in fractionated sediment indicated by the apparent partition coefficients showed no significant difference for different fractions. Thus, size and density separation does not help to understand the desorption resistance of HOCs in contaminated sediments due to the absence of ease to separated amorphous and condensed phase organic carbon completely from the sediment.

- Chemical analysis of coarse particles from different sediments showed great variation in concentrations of PAHs, with total PAHs concentration up to 2,735 mg/Kg. Generally, PAHs concentrations in coarse particles were significantly higher than those in corresponding whole sediments. This was in good agreement with observations reported in Ghosh et al. (2000) and Jonker et al (2002) that PAHs contamination in sediments was predominantly associated with black particles.

- Phenanthrene adsorption experiment onto coarse particles showed various sorption rates. Slow sorption rate was observed for coal-like particles. Difficulty for diffusion of phenanthrene into coal-like particles was most likely the reason leading to the slow adsorption rate.

- Apparent partition coefficients of PAHs associated with coal cinder particles under basic condition were roughly equal to those under neutral condition, which was contrary to coal-like particles. Apparent partition coefficients of PAHs associated with coal-like particles under basic condition were significantly less than those under neutral condition. It was most likely due to

dissolution of amorphous organic carbon from coal-like particles such as humic acid into aqueous phase under basic condition.

- The apparent partition coefficients of PAHs in condensed phase organic carbon particles were a good indication of the apparent partition coefficients in the bulk Utica Harbor and Rouge River sediment. The apparent partition coefficients of contaminants in bulk Utica Harbor sediment were not linear combination of the apparent partition coefficients for the amorphous and condensed phase organic carbon according to the amorphous and condensed phase organic carbon contents because the apparent partition coefficients were not determined in true equilibria.

- Both kinetics and equilibrium effect are included in the model to study the transport and sequestration of contaminants in sediments. The ability of the model to predict sorption/desorption behavior of HOCs in contaminated sediments suggest that slow diffusion process of HOCs in condensed phase carbon in sediment is most likely the reason leading to the biphasic desorption behavior and observed desorption resistance.

- The model is able to predict biphasic desorption, desorption resistance and aging effect of PAHs in laboratory-contaminated sediments. The best fit results for diffusivity of phenanthrene in condensed phase organic matter was $2.2*10^{-17}$ m^2/s and volume to surface area ratio was $2.0*10^{-5}$m.

- The model is able to model fast desorption fraction and apparent partition coefficients of PAHs in field-contaminated sediments, with diffusivity in

condensed phase carbon of $1.8\sim2.2*10^{-19}$ m^2/s for different compounds and volume/surface area of $1.5*10^{-5}$ m.

Recommendations:

The current work established the model to successfully address physical availability of PAHs as representative hydrophobic organic contaminants in sediments. Several future areas suggested by our results are summarized below.

- Explore other HOCs such as PCBs, chlorinated pesticides etc. other than PAHs

- Current model to be coupled with conceptual model proposed by Lu 2003 to estimate bioavailability

- Characterization of amorphous and condensed phase organic matter using NMR

REFERENCES

1. Accardi-Dey A. and Gschwend, P. M., 2002, Assessing the Combined Roles of Natural Organic Matter and Black Carbon as Sorbents in Sediments, *Environ. Sci. & Technol.*, 36, 21-29.

2. Accardi-Dey A. and Gschwend, P. M., 2003, Reinterpreting Literature Sorption Data Considering Both Absorption into Organic Carbon and Adsorption onto Black Carbon, *Environ. Sci. & Technol.*, 37, 99-106.

3. Adamson, A.W., 1990, *Physical Chemistry of Surfaces*, 5th ed., John Wiley & Sons, Inc., New York.

4. Ahmad, R., Kookana, R. S., Alston, A. M. and Skjemstad, J. O., 2001, The Nature of Soil Organic Matter Affects Sorption of Pesticides. 1. Relationships with Carbon Chemistry as Determined by 13C CPMAS NMR Spectroscopy, *Environ. Sci. & Technol,* 35, 878-884.

5. Allen-King, R. M., Grathwohl, P. and Ball, W. P., 2002, New Modeling Paradigms for the Sorption of Hydrophobic Organic Chemicals to Heterogeneous Carbonaceous Matter in Soils, Sediments and Rocks, *Advances in Water Resources*, 25, 985-1016.

6. Ball, W. P., Roberts, P. V., 1991, Long-term sorption of halogenated organic chemicals by aquifer material. 1. Equilibrium, *Environ. Sci. & Technol.* 25, 1223-1237.

7. Ball, W. P., Roberts, P. V., 1991, Long-term sorption of halogenated organic chemicals by aquifer material. 2. Intraparticle diffusion, *Environ. Sci. & Technol.* 25, 1237-1249.

8. Braida, W. J., Pignatello, J. J., Lu, Y., Ravikovitch, P. I., Neimark, A. V. and Xing, B., 2003, Sorption Hysteresis of Benzene in Charcoal Particles, *Environ Sci. & Technol.,* 37, 409-417.

9. Bucheli, T. D. and Gustafsson, Ö., 2000, Quantification of the Soot-Water Distribution Coefficient of PAHs Provides Mechanistic Basis for Enhanced Sorption Observations, *Environ. Sci. & Technol.*, 34, 5144-5151.

10. Burgos, W. D., Novak, J. T. and Berry, D. F., 1996, Reversible Sorption and Irreversible Binding of Naphthalene and α-Naphthol to Soil: Elucidation of Processes, *Environ. Sci. & Technol,* 30, 1205-1211.

11. Carroll, K. M., Harkness, M. R., Bracco, A. A. and Balcarcel, R. R., 1994, Application of a Permeant/Polymer Diffusional Model to the Desorption of Polychlorinated Biphenyls from Hudson River Sediments, *Environ. Sci. & Technol,* 28, 253-258.

12. Chefetz, B., Deshmukh, A. Hatcher, P. G. and Guthrie, E. A., 2000, Pyrene Sorption by Natural Organic Matter, *Environ. Sci. & Technol.*, 34, 2956-2930.

13. Chen, W., Kan, A. T. and Tomson, M. B., 2000, Irreversible Adsorption of Chlorinated Benzenes to Natural Sediments: Implications for Sediment Quality Criteria. *Environ. Sci. Technol.* 34, 385-392.

14. Chen, W., Kan, A. T., Fu, G., Vignona, L. C. and Tomson, M. B., 1999, Adsorption-Desorption Behaviors of Hydrophobic Organic Compounds in Sediments of Lake Charles, LA, USA. *Environmental Toxicology and Chemistry*, 18, 1610-1616.

15. Chen, Z., Xing, B., McGill, W. B. and Dudas, M. J., 1996, α-Naphthol Sorption as Regulated by Structure and Composition of Organic substances in Soils and Sediments, *Canadian Journal of Soil Science*, 513-522.

16. Chiou, C. T. McGroddy, S. E. and Kile D. E., 1998, Partition Characteristics of Polycyclic Aromatic Hydrocarbons on Soils and Sediments, *Environ. Sci. & Technol.*, 32, 264-269.

17. Chiou, C. T., Kile, D. E., Rutherford, D. W., Sheng, G. and Boyd, S. A., 2000, Sorption of Selected Organic Compounds from Water to a Peat Soil and Its Humic-Acid and Humin Fractions: Potential Sources of the Sorption Nonlinearity, *Environ. Sci. & Technol.,* 34, 1254-1258.

18. Connaughton, D. F., Stedinger, J. R. Lion, L. W., and Shuler, M. L., 1993, Description of Time-Varying Desorption Kinetics: Release of Naphthalene from Contaminated Soils, *Environ. Sci. & Technol,* 27, 2397-2403.

19. Cornelissen, G., Rigterink, H., Hulscher, D. E.M.T., Vrind, B. A. and Van Noort, P. C. M., 2001, A Simple TENAX Extraction Method to Determine the Availability of Sediment-Sorbed Organic Compounds, *Environmental Toxicology and Chemistry*, 20, 706-711.

20. Cornelissen, G., Van Noort, P. C. M., Nachtegaal, G. and Kentgens A. P. M., 2000, A Solid-State Fluorine-NMR Study on Hexafluorobenzene Sorbed by Sediments, Polymers, and Active Carbon, *Environ. Sci. & Technol.*, 34, 645-649.

21. Crank, J, 1975, *The Mathematics of Diffusion*, 2nd Ed, Clarendon Press, Oxford.

22. Crank, J. and Park, G. S., 1968, *Diffusion in Polymers*, Academic Press, London and New York.

23. Cunningham, R. E. and Williams, R. J. J., 1980, *Diffusion in Gases and Porous Media*, Plenum Press. New York and London.

24. Devitt, E. C. and Wiesner, M. R., 1998, Dialysis Investigations of Atrazine-Organic Matter Interactions and the Role of a Divalent Metal, *Environ. Sci. & Technol,* 32, 232-237.

25. Fu, G., Kan, A. T. and Tomson, M., 1994, Adsorption and Desorption Hysteresis of PAHs in Surface Sediment. *Environmental Toxicology and Chemistry*, 13, 1559-1567.

26. Gaboriau H. and Saada, S., 2001, ?????, Chemosphere, 44, 1633-1639.

27. Ghosh, U., Gillette, J. S., Luthy, R. G. and Zare, R. N., 2000, Microscale Location, Characterization, and Association of PAH on Harbor Sediment Particles, *Environ. Sci. & Technol.*, 34, 1729-1736.

28. Ghosh, U., Simmerman, J. R. and Luthy R. G., 2003, PCB and PAH Speciation among Particle Types in Contaminated Harbor Sediments and Effects on PAH Bioavailability, *Environ. Sci. & Technol.*, 37, 2209-2217.

29. Ghosh, U., Talley, J. W. and Luthy, R. G., 2001, Particle-Scale Investigation of PAH Desorption Kinetics and Thermodynamics from Sediment, *Environ. Sci. & Technol.*, 35, 3468-3475.

30. Gillette, J. S., Luthy, R. G., Clemett, S., and Zare, R.N., 1999, Direct Observation of PAH on Geosorbents at the Subparticle Scale, *Environ. Sci. & Technol.*, 33, 1185-1192

31. Graber, E.R. and Borisover, M.D., 1998, Evaluation of the Glassy/Rubbery Model for Soil Organic Matter. *Environ. Sci. & Technol.*, 32, 3286-3292.

32. Gregg, S. J., Sing, K.S.W., 1982, *Adsorption, Surface Area and Porosity*; Academic Press, London.

33. Gustafsson, Ö. and Gschwend, P. M., 1997, In Molecular Markers in Environmental Geochemistry; Eganhouse, R.P., Ed., ACS Symposium Series 671; American Chemical Society, Washington DC, pp 365-381.

34. Gustafsson, Ö., Haghseta, F., Chan, C., Macfarlane, J. and Gschwend, P. M., 1997, Quantification of the Dilute Sedimentary Soot Phase: Implications for PAH Speciation and Bioavailability, *Environ. Sci. & Technol.*, 31, 203-209.

35. Hatzinger, P. B. and Alexander, M., 1995, Effect of Aging of Chemicals in Soil on Their Biodegradability and Extractability, *Environ. Sci. & Technol.*, 29, 537-545.

36. Hawthorne, S. B., Poppendieck, D. G., Grabanski, C. B. and Loehr R. C., 2001, PAH Release during Water Desorption, Supercritical Carbon Dioxide Extraction, and Field Bioremediation, *Environ. Sci. & Technol.*, 35, 4577-4583.

37. Hawthorne, S. B., Poppendieck, D. G., Grabanski, C. B. and Loehr R. C., 2002, Comparing PAH Availability from Manufactured Gas Plant Soils and Sediments with Chemical and Biological Tests. 1. PAH Release during Water Desorption, Supercritical Carbon Dioxide Extraction, *Environ. Sci. & Technol.*, 36, 4795-4803.

38. Huang, W. and Weber, W. J., Jr., 1997a, A Distributed Reactivity Model for Sorption by Soils and Sediments. 10. Relationships between Desorption, Hysteresis, and the Chemical Characteristics of Organic Domains, *Environ. Sci. & Technol.*, 31, 2562-2569.

39. Huang, W. and Weber, W. J., Jr., 1997b, Thermodynamics Considerations in the Sorption of Organic Contaminants by Soils and Sediments. 1. The Isosteric Heat Approach and Its Application to Model Inorganic Sorbents, *Environ. Sci. & Technol,* 31, 3238-3243.

40. Huang, W. and Weber, W. J., Jr., 1998, A Distributed Reactivity Model for Sorption by Soils and Sediments. 11. Slow Concentration-Dependent Sorption Rates, *Environ. Sci. & Technol.*, 32, 3549-3555.

41. Huang, W., 1997. Sorption and Desorption by Soils and Sediments: Effects of Sorbent Heterogeneity. Ph.D. dissertation, The University of Michigan, Ann Arbor, MI.

42. Huang, W., Schlautman M. A. and Weber, W. J., Jr., 1996, A Distributed Reactivity Model for Sorption by Soils and Sediments. 5. The Influence of Near-Surface Characteristics in Mineral Domains, *Environ. Sci. & Technol.*, 30, 2993-3000.

43. Huang, W., Young, T., Schlautman, M. A., Yu, H. and Weber, W. J., 1996, A Distributed Reactivity Model for Sorption by Soils and Sediments. 9. General Isotherm Nonlinearity and Applicability of the Dual Reactive Domain Model, *Environ. Sci. & Technol.*, 31, 1703-1710.

44. Hunter, M. A, Kan, A. T., and Tomson, M. B., 1996, Development of a Surrogate Sediment To Study the Mechanisms Responsible for Adsorption/Desorption Hysteresis. *Environ Sci. & Technol.*, 30, 2278-2285.

45. Johnson, M. D. and Weber, W. J., Jr., 2001, Rapid Prediction of Long-Term Rates of Contaminant Desorption from Soils and Sediments, *Environ. Sci. & Technol,* 35, 427-433.

46. Johnson, M. D., Huang, W. and Weber, W. J., Jr., 2001, A Distributed Reactivity Model for Sorption by Soils and Sediments. 13. Simulated Diagenesis of Natural Sediment Organic Matter and Its Impact on Sorption/Desorption Equilibria, *Environ. Sci. & Technol.*, 35, 1680-1687.

47. Johnson, M. D., Huang, W., Dang, Z. and Weber, W. J., Jr., 1999, A Distributed Reactivity Model for Sorption by Soils and Sediments. 12. Effects of Subcritical Water Extraction and Alterations of Soil Organic Matter on Sorption Equilibria, *Environ. Sci. & Technol.*, 33, 1657-1663.

48. Johnson, M. D., Keinath, T. M. II and Weber, W. J., Jr., 2001, A Distributed Reactivity Model for Sorption by Soils and Sediments. 14.Characterization and Modeling of Phenanthrene Desorption Rates, *Environ. Sci. & Technol,* 35, 1688-1695.

49. Jonker, M. T. O. and Koelmans, A. A., 2002, Sorption of Polycyclic Aromatic Hydrocarbons and Polychlorinated Biphenyls to Soot and Soot-like Materials in the Aqueous Environment: Mechanistic Considerations, *Environ. Sci. & Technol,* 36, 3725-3734.

50. Jonker, M. T. O. and Smedes, F., 2000, Preferential Sorption of Planar Contaminants in Sediments from Lake Ketelmeer, The Netherlands, *Environ. Sci. & Technol.*, 34, 1620-1626.

51. Kan, A. T., Fu, G. and Tomson, M. B., 1994, Adsorption/Desorption Hysteresis in Organic Pollutant and Soil/Sediment Interaction. *Environ Sci. & Technol.*, 28, 859-867.

52. Kan, A. T., Fu, G., Hunter, M. A., and Tomson, M. B., 1997, Irreversible Adsorption of Naphthalene and Tetrachlorobiphenyl to Lula and Surrogate Sediments. *Environ Sci. & Technol.*, 31, 2176-2185

53. Kan, A. T., Fu, G., Hunter, M., Chen, W., Ward, C. H., and Tomson, M. B., 1998, Irreversible Adsorption of Neutral Hydrocarbons to Sediments: Experimental Observations and Model Predictions. *Environ Sci. & Technol.*, 32, 892-902.

54. Kan, A.T., Chen, W., Tomson, M.B., 2000, Desorption Kinetics of Neutral Hydrophobic Organic Compounds from Field-contaminated sediment. *Environmental Pollution*, 108, 81-89.

55. Karapanagioti, H. K. and Sabatini, D. A., 2000, Impacts of Heterogeneous Organic Matter on Phenanthrene Sorption: Different Aquifer Depths, *Environ. Sci. & Technol,* 34, 2453-2460.

56. Karapanagioti, H. K., Childs, J. and Sabatini, D. A., 2001, Impacts of Heterogeneous Organic Matter on Phenanthrene Sorption: Different Soil and Sediment Samples, *Environ. Sci. & Technol,* 35, 4684-4690.

57. Karapanagioti, H.K., Keineidm, S., Sabatini, D.A., Grathwohl, P. and Ligouis, B., 2000, ??????? *Environ. Sci. & Technol.*,34,406-414.

58. Karickhoff, S. W., 1980, Sorption Kinetics of Hydrophobic Pollutants in Natural Sediments, In *Contaminants and Sediments*; Vol. 2, Edited by Baker, R. A. Ann Arbor Science Publishers, Ann Arbor, MI, 193-205.

59. Karickhoff, S. W., and Morris, K. R., 1985, Sorption Dynamics of Hydrophobic Pollutants in Sediment Suspensions, *Environmental Toxicology and Chemistry*, 4, 469-479.

60. Karickhoff, S. W., Brown, D. S. and Scott, T. A., 1979, Sorption of Hydrophobic Pollutants on Natural Sediments, *Water Research*, 13, 241-248.

61. Karimi-Lotfabad, S., Pickard, M. A. and Gray, M. R., 1996, Reactions of Polynuclear Aromatic Hydrocarbons on Soil, *Environ. Sci. & Technol,* 30, 1145-1151.

62. Kile, D. E., Chiou, C. T., Zhou, H., Li, H. and Xu, O., 1995, Partitioning of Nonpolar Organic Pollutants from Water to Soil and Sediment Organic Matters, *Environ. Sci. & Technol.*, 29, 1401-1406.

63. Kile, D. E., Wershaw, R. L. and Chiou, C. T., 1999, Correlation of Soil and Sediment Organic Matter Polarity to Aqueous Sorption of Nonionic Compounds, *Environ. Sci. & Technol.*, 33, 2053-2056.

64. Kubicki, J. D. and Apitz, S. E., 1999, Models of Natural Organic Matter and Interactions with Organic Contaminants, *Organic Geochemistry*, 30, 911-927.

65. Lahlou, M. and Ortega-Calvo, J. J., 1999, Bioavailability of Labile and Desorption-Resistant Phenanthrene Sorbed to Montmoriallonite Clay Containing Humic Fractions, *Environmental Toxicol. and Chemistry*, 18(12), 2729-2735.

66. Laor, Y. and Rebhun, M., 2002, Evidence for Nonlinear Binding of PAHs to Dissolved Humic Acids, *Environ. Sci. & Technol,* 36, 955-961.

67. Leboeuf, E. J. and Weber, W. J., Jr., 1997, A Distributed Reactivity Model for Sorption by Soils and Sediments. 8. Sorbent Organic Domains: Discovery of a Humic Acid Glass Transition and an Argument for a Polymer-Based Model, *Environ. Sci. & Technol.*, 31, 1697-1702.

68. Leboeuf, E. J. and Weber, W. J., Jr., 2000, Macromolecular Characteristics of Natural Organic Matter. 1.Insights from Glass Transition and Enthalpic Relaxation Behavior, *Environ. Sci. & Technol,* 34, 3623-3631.

69. Lee, S., 2001. Biodegradation of Desorption-Resistant Organic Contaminants in Wetland Soils, *Ph.D. Dissertation*, Louisiana State University, Baton Rouge, LA, USA.

70. Lu, X.X., 2003a, Bioavailability And Bioaccumulation Of Sediment-Associated, Desorption-Resistant Fraction Of Polycyclic Aromatic Hydrocarbon Contaminants, *Ph.D. Dissertation*, Louisiana State University, Baton Rouge, LA, USA.

71. Lu, X.X., Reible, D.D., Fleeger, J.W., Chai, Y.Z., 2003b. Bioavailability of desorption–resistant phenanthrene to Oligochaete, *Ilyodrilus templetoni*, 22,153-160.

72. Lu, Y. and Pignatello, J. J., 2002, Demonstration of the "Conditioning Effect" in Soil Organic Matter in Support of a Pore Deformation Mechanism for Sorption Hysteresis, *Environ Sci. & Technol.,* 36, 4553-4561.

73. Luthy, R. G., Aiken, G., Brusseau, M. L., Cunningham, S. D., Gschwend, P. M., Pignatello, J. J., Reinhard, M., Traina, S. J., Weber, W. J., Jr. and Westall, J. C., 1997,

Sequestration of Hydrophobic Organic Contaminants by Geosorbents, *Environ. Sci. & Technol.*, 31, 3341-3347.

74. Ma, L., Southwick, L. M., Willis, G. H., and Selim, H. M., 1993, Hysteresis Characteristics of Atrazine Adsorption-Desorption by a Sharkey Soil, *Weed Science,* 41, 627-633.

75. Mackay, D., Shiu, W. Y., and Ma, K. C., 1991, Illustrated Handbook of Physical-Chemical Properties and Environmental Fate for Organic Chemicals, Vol. II, Polynuclear Aromatic Hydrocarbons, Polychlorinated Dioxins, and Dibenzofurans.

76. Maruya, K. A., Risebrough, R. W. and Horne, A. J., 1996, Partitioning of Polynuclear Aromatic Hydrocarbons between Sediments from San Francisco Bay and Their Porewaters, *Environ. Sci. & Technol.*, 30, 2942-2947.

77. Mayer, L. M., Jumars, P. A., Taghon, G. L., Macko, S. A., Trumbore, S., 1993, (Article title) *Journal of Marine Research*, 51, 373-389.

78. McGinley, P. M., and Katz, L. E., Weber, W. J., Jr., 1993, A Distributed Reactivity Model for Sorption by Soils and Sediments. 2. Multicomponent Systems and Competitive Effects, *Environ. Sci. & Technol.*, 27, 1524-1531.

79. McGroddy, S. E. and Farrington, J. W., 1995, Sediment Porewater Partitioning of Polycyclic Aromatic Hydrocarbons in Three Cores from Boston Harbor, Massachusetts, *Environ. Sci. & Technol,* 29, 1542-1550.

80. McGroddy, S. E., Farrington, J. W. and Gschwend, P. M., 1996, Comparison of the *in Situ* and Desorption Sediment-Water Partitioning of Polycyclic Aromatic Hydrocarbons and Polychlorinated Biphenyls, *Environ. Sci. & Technol.*, 30, 172-177.

81. Northcott, G. L. and Jones, K. C., 2001, Partitioning, Extractability, and Formation of Nonextractable PAH Residues in Soil. 1. Compound Differences in Aging and Sequestration, *Environ. Sci. & Technol,* 35, 1103-1110.

82. Northcott, G. L. and Jones, K. C., 2001, Partitioning, Extractability, and Formation of Nonextractable PAH Residues in Soil. 2. Effects on Compound Dissolution Behavior, *Environ. Sci. & Technol,* 35, 1111-1117.

83. Pedit, J. A. and Miller, 1996, Comment on "A Distributed Reactivity Model for Sorption by Soils and Sediments. 4. Intraparticle Heterogeneity and Phase-Distribution Relationships under Nonequilibrium Conditions", *Environ. Sci. & Technol,* 30, 3128-3129.

84. Pignatello, J. J. and Xing, B., 1996, Mechanisms of Slow Sorption of Organic Chemicals to Natural Particles, *Environ. Sci. & Technol.*, 30, 1-11.

85. Pignatello, J. J., Ferrandino, F. J. and Huang L. Q., 1993, Elution of Aged and Freshly Added Herbicides from a Soil, *Environ. Sci. & Technol.,* 27, 1563-1571.

86. Rockne, K. J., Shor, L. M., Young, L.Y., Taghon, G. L. and Kosson, D. S., 2002, Distributed Sequestration and Release of PAHs in Weathered Sediment: The Role of Sediment Structure and Organic Carbon Properties, *Environ. Sci. & Technol.*, 36, 2636-2644.

87. Rockne, K. J., Taghon, G. L. and Kosson, D. S., 2000, Pore Structure of Soot Deposits from Several Combustion Sources, *Chemosphere*, 41, 1125-1135.

88. Salloum, M.J., Chefetz, B., Hatcher, P.G., 2002, ?????? *Environ. Sci. & Technol.*, 36, 1953-1958.

89. Shor, L. M., Liang, W., Rockne, K. J., Young, L.Y., Taghon, G. L. and Kosson, D. S., 2003, Intra-Aggregate Mass Transport-Limited Bioavailability of Polycyclic Aromatic Hydrocarbons to Mycobacterium Strain PC01, *Environ. Sci. & Technol.*, 37, 1545-1552.

90. Shor, L.M., Rockne, K.J., Taghon, G.L., Young, L.Y. and Kosson, D.S., 2003, Desorption Kinetics for Field-Aged Polycyclic Aromatic Hydrocarbons from Sediments, *Environ. Sci. & Technol.,* 37, 1535-1544.

91. Talley, J. W., Ghosh, U., Tucker, S. G., Furey, J. S. and Luthy, R. G., 2002, Particle-Scale Understanding of the Bioavailability of PAHs in Sediment, *Environ. Sci. & Technol.*, 36, 477-483.

92. USEPA, May 1996. Soil Screening Guidance Technical Background Document. EPA/540/R-95/128.

93. Walters, R. W. and Luthy, R. G., 1984, Equilibrium Adsorption of Polycyclic Aromatic Hydrocarbons from water onto Activated Carbon, *Environ. Sci. & Technol.*, 18, 395-403.

94. Weber, W. J., Jr. and Huang, W., 1996, A Distributed Reactivity Model for Sorption by Soils and Sediments. 4. Intraparticle Heterogeneity and Phase-Distribution Relationships under Nonequilibrium Conditions, *Environ. Sci. & Technol.*, 30, 881-888.

95. Weber, W. J., Jr. and Young, T., 1997, A Distributed Reactivity Model for Sorption by Soils and Sediments. 6. Mechanistic Implications of Desorption under Supercritical Fluid Conditions, *Environ. Sci. & Technol.*, 31, 1686-1691.

96. Weber, W. J., Jr., Kim, S. H. and Johnson, M. D., 2002, Distributed Reactivity Model for Sorption by Soils and Sediments. 15. High-Concentration Co-Contaminant Effects on Phenanthrene Sorption and Desorption, *Environ. Sci. & Technol,* 36, 3625-3634.

97. Weber, W. J., Jr., McGinley, P. M. and Katz, L. E., 1992, A Distributed Reactivity Model for Sorption by Soils and Sediments. 1. Conceptual Basis and Equilibrium Assessments, *Environ. Sci. & Technol.*, 26, 1955-1962.

98. White, J. C. and Pignatello, J. J., 1999, Influence of Bisolute Competition on the Desorption Kinetics of Polycyclic Aromatic Hydrocarbons in Soil, *Environ. Sci. & Technol.*, 33, 4292-4298.

99. White, J. C., Alexander, M. and Pignatello, J. J., 1999, Enhancing the Bioavailability of Organic Compounds Sequestration in Soil and Aquifer Solids, *Environ Toxicol. And Chemistry,* 18(2), 182-187.

100. White, J. C., Hunter, M., Pignatello, J. J. and Alexander, M., 1999, Increase in Bioavailability of Aged Phenanthrene in Soils by competitive displacement with Pyrene, *Environ Toxicol. And Chemistry*, 18, 1728-1732.

101. White, J. C., Kelsey, J. W., Hatzinger, P. B. and Alexander, M., 1997, Factors Affecting Sequestration and Bioavailability of Phenanthrene in Soils, *Environmental Toxicology and Chemistry*, 16, 2040-2045.

102. White, J.C., Riverta, A.Q., Alexander, M., 1998, Effect of wetting and drying on the bioavailability of organic compounds sequestered in soil. *Environmental Toxicology and Chemistry*, 17, 2378-2382

103. Wu, S. and Gschwend, P. M., 1986, Sorption Kinetics of Hydrophobic Organic Compounds to Natural Sediments and Soils, *Environ. Sci. & Technol,* 20, 717-725.

104. Xing, B. and Pignatello, J. J., 1996 (a), Time-Dependent Isotherm Shape of Organic Compounds in Soils Organic Matter: Implications for Sorption Mechanism, *Environ Toxicology and Chemistry*, 15, pp 1282-1288.

105. Xing, B. and Pignatello, J. J., 1997, Dual-Mode Sorption of Low-Polarity Compounds in Glassy Poly(Vinyl Chloride) and Soil Organic Matter, *Environ. Sci. & Technol.*, 31, 792-799.

106. Xing, B. and Pignatello, J. J., 1998, Competitive Sorption between 1,3-Dichlorobenzene or 2,4-Dichlorophenol and Natural Aromatic Acids in Soil Organic Matter, *Environ. Sci. & Technol.*, 32, 614-619.

107. Xing, B., Pignatello, J. J., and Gigliotti, B., 1996 (b), Competitive Sorption between Atrazine and other Organic Compounds in Soils and Model Sorbents. *Environ. Sci. & Technol.*, 30, 2432-2440.

108. Young, T. and Weber, W. J., Jr., 1997, A Distributed Reactivity Model for Sorption by Soils and Sediments. 7. Enthalpy and Polarity Effects on Desorption under Supercritical Conditions, *Environ. Sci. & Technol.*, 31, 1692-1696.

109. Young, T. M. and Weber, W. J., Jr., 1995, A Distributed Reactivity Model for Sorption by Soils and Sediments. 3. Effects of Diagenetic Processes on Sorption Energetics, *Environ. Sci. & Technol.*, 29, 92-97.

APPENDICES

       I. COMPUTATIONAL METHOD FOR THE MODEL

     II. MATLAB CODE FOR THE MODEL

    III. NOMENCLATURE

VITA

Mr. Yunzhou Chai was born in the winter of 1975 in a tiny village of Cili, Hunan, P. R. China, a mountainous village in the vicinity of the fantastic Wulinyuan scenic region in Zhangjiajie, Hunan, which is one of the world heritages located in central southern China. He lived in the village until he finished middle school. He went to the Cili No. 1 High School which was located in the county of Cili, Hunan and spent three years there.

In the fall of 1993, he traveled to Xiamen, Fujian, for his higher education, which had been in his dream for many years. He graduated from Xiamen University in July 1997, with a Bachelor of Science degree in chemical engineering. He spent almost two years toward his Master's degree in Xiamen University before he actually got the degree.

In August 1999, he flew over the Pacific Ocean to attend the graduate program in Chemical Engineering at Louisiana State University, working toward a doctor degree, which will be conferred in December 2004.